Inherited p40phox deficiency differs from classic chronic granulomatous disease

DOI:
10.1172/JCI97116

Document Version
Accepted author manuscript

Point-by-point responses to the referees

97116-JCI-RG-DN-2, Inherited p40phox deficiency is related to but different from classical chronic granulomatous disease.

COMMENTS FROM REVIEWER A:

The new version of "Inherited p40phox deficiency is different from chronic granulomatous disease: distinctive molecular, cellular and clinical phenotypes" by van de Geer et al. (97116-JCI-RG-DN2) contributes important and novel insights into our understanding of the clinical consequences of defects in the human neutrophil NADPH oxidase. In general, the authors have improved the organization of the manuscript, which is a notable accomplishment, given the large amount of information presented. Furthermore, refinements in the grammar and diction have improved the clarity of the presentation.
Responses to critique of original submission: The authors provide thoughtful and throrough responses to my comments about their initial submission (Reviewer #1). On point #5 (opsonized zymosan vs E.coli as a diagnostic tool to screen oxidase activity), I thank the authors for the explanation of their rationale. I stand corrected.
New issues: As anticipated, a thoroughly revised and reorganized manuscript elicits new concerns and comments.

We very much appreciate the interest and suggestions of the referee in our study.

1) The change in title and the recurrent text contrasting p40phox deficiency with CGD need to be reassessed and, in my opinion, corrected. Rather than suggesting that p40phox deficiency is distinct from CGD, I see p40phox deficiency as a variant of CGD (a clinical disorder caused by abnormalities in the phagocyte NADPH oxidase) that has some distinct features that differ from those of CGD due to defects in gp91phox, p22phox, p47phox or p67phox. In fact, whereas the opening sentence of the abstract suggests that CGD reflects defects in 4 (of the 5) oxidase components, the initial sentence of Introduction correctly states that abnormalities of any of the five components of the NADPH oxidase underlie the clinical disorder CGD. It would be easy to correct the text; for example (line 12, page 7), "differences between p40phox deficiency and other forms of CGD:

We agree with the referee and have revised the manuscript and the title accordingly.

2) Inclusion of some of the seminal discoveries related to CGD is a welcome feature of the Introduction.

a) However, CGD was first described by Charles Janeway in the account of Society Transactions of the American Pediatric Society held May 1954 and published by AMA American Journal of Diseases of Childhood. CGD was first reported in an article in 1959 (Bridges et al Am J Dis Child 97:387, 1959) and first linked to defective neutrophil function in 1966 (Holmes et al. Lancet 1:1225, 1966).

We agree with the referee and have revised the manuscript accordingly.

b) Oddly, the authors highlight gp91phox identification but overlook the discovery of p47phox and p67phox, abnormalities of which account for ~30% of patients with CGD. The discoveries that cytosolic factors are required for NADPH oxidase activity and that their absence causes CGD were major advances in understanding normal phagocyte activity and the molecular basis for some forms of CGD.

We agree with the referee and have revised the manuscript accordingly

3. Whereas the authors followed the convention in scientific writing to use the present tense of verbs when discussing published work in most of the manuscript, the last paragraph of the Introduction uses the past tense. This error should be corrected.

We apologize for this error, which has been corrected.

4. The major insight that p40phox deficiency brings to the understanding of the normal NADPH oxidase (nicely illustrated in reference 28) is the essential role of p40phox in the assembly of the oxidase on phagosomes (vs plasma membrane). Text on the bottom of page 15 and top of page 16 seems off the mark in emphasizing that "p40phox-dependent pathway activates the NADPH oxidase complex in response to these microorganisms". Membrane recruitment of p40phox to the phagosome is the point to emphasize, not the contents of the phagosome, which are not likely to alter p40phox recruitment.

We agree with the referee and have revised the manuscript accordingly.

5. The authors overstate the relative differences in the prevalence of gastrointestinal disease in p40phox deficiency and typical CGD (page 19). In this report, 6 of 24 patients (25%) exhibit features that resemble those of Crohn's disease. In typical CGD, up to 40% of patients have IBD-like disease and 18% of CGD patients present with IBD-like symptoms (Kangura et al. Clin Gastro Hepat 14:395, 2016). I think that the text should be more measured to be in line with the literature.

We thank the referee for this important remark. We have revised the manuscript accordingly. See revised manuscript page 23

6. The text discussing outcome (pages 20-21) needs refinement. The comprehensive study of Kuhns et al. (ref 20) demonstrates that prognosis parallels the residual capacity to generate superoxide activity. In addition, neutrophils of patients with CGD due to absence of functional gp91phox have profoundly depressed oxidant generation and a worse prognosis, both features that contrast with the significant residual oxidase activity and better prognosis in the context of CGD due to defects in p47phox. As I see the data, the residual activity and better prognosis of p40phox deficiency mirror what is seen in p47phox deficiency. Comparing the prognosis of all forms of "typical" CGD (which includes the severe situation due to gp91phox deficiency) misleads the reader. A more comprehensive comparison that compares residual superoxide generation and prognosis of the

cytosolic factor deficiencies (p47, p67, and p40) should be done. In addition, the data in reference 6 were published nearly 20 years ago; more recent outcome data (e.g. in ref 20) should be used for comparisons.

We agree with the referee and have revised the manuscript accordingly. In our revised Figure 7C, we have separated the CGD patients in AR and XL forms to give a better comparison. Additionally, we have included data from a Turkish cohort from 2013 (Köker M.Y., *et al,* JACI, 2013). Unfortunately, we could not obtain the raw data from ref 18 (Kunhs D.B. *et al*, NEJM 2010) (Figure 1A) and ref 10 (Van den Berg, J.M. *et al*, PLoS One 2009) (Figure 1B). Nevertheless, when comparing CGD (XL, AR) vs p40^{phox} deficiency all curves showed the same tendency as the one we used for the revised manuscript (Figure 1C).

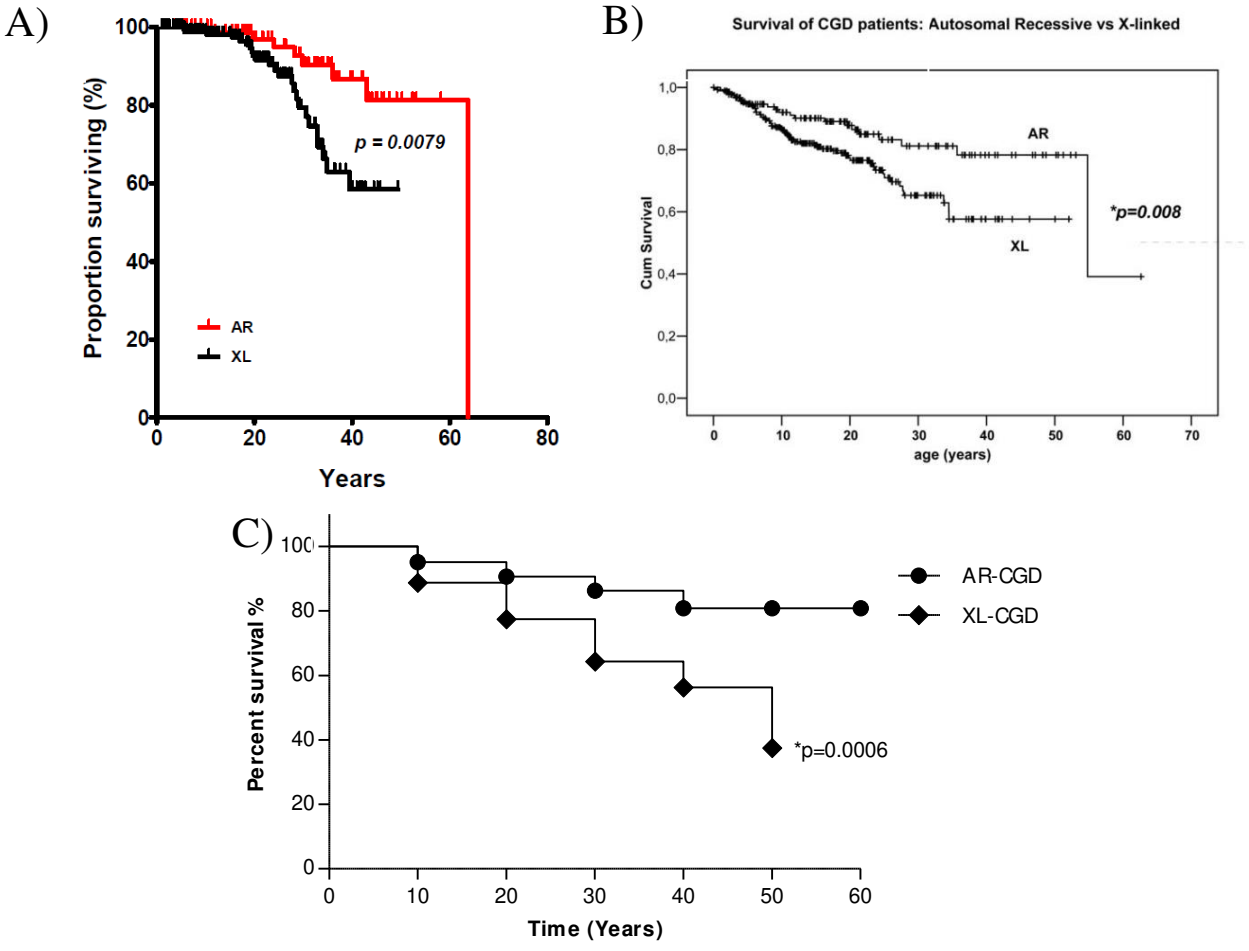

FIGURE 1. A) Survival curve of 287 CGD patients (XL n=195; AR n=92). B) Survival curve of 429 CGD patients (XL n=290; AR n=139). C) Survival curve of 363 CGD patients (XL n=240; AR n=123)

COMMENTS FROM REVIEWER B:

The manuscript has been revised according to the comments of the reviewer. The revised version is a very careful study investigating a large group of patients, and pointing out an important mechanism - both mechanistically and diagnostically.

We very much appreciate the referee's interest in our study.

Minor point - Fig4 CGD group - due to the small bar it is only possible to guess the group affiliation of CGD due to the order of the bars. The open white bar might not be the best choice for this bar.

We agree with the referee and have revised the figure accordingly. See new Supplemental Figure 5.

COMMENTS FROM REVIEWER C:

The revised manuscript is considerably improved. The study now very clearly communicates the cellular and clinical phenotypic divergence between CGD and p40phox deficiency, and presents a rigorous experimental analysis that defines the mechanistic basis for the loss of cellular function in p40phox deficiency. These findings represent an important clinical advance that will be of broad interest; similarly, it is anticipated that these will shape immunodeficiency diagnosis and inform patient management.

We very much appreciate the referee's interest in our study.

List of incorporated changes:

Title:

Inherited p40phox deficiency differs from classic chronic granulomatous disease. On request of Reviewer A and following JCI recommendations (word limit 10)

Introduction:

Page 6: Inclusion of refs (2) (6) on request of Reviewer A

Results:

Pages 8-20**:** Reduction of the text from 3,994 to 3,619 words

Page 9: Inclusion of founder effect analysis in two Latin American patients carrying the c.172C>T (p.R58C) mutation

Page 11: Inclusion of new data in EVB-B cells virally transduced with two *NCF4* alleles: c.118_198del, p.Asp254Serfs96*

Page 19: Inclusion of recent data ref (19) for Kaplan Meier curves on request of Reviewer A comment 6

Discussion:

Page 21: Inclusion of ref (48) in response to Reviewer A Comment 5.

Page 22: Revised conclusion from Kaplan Meier curves on request of Reviewer A comment 6

Methods

Page 29: Inclusion of detailed description of statistical analysis.

Page 30: Inclusion of Study approval section.

Figures

None of the previous figures were eliminated in the revised version but were re-ordered on request of the Editors.

Previous Figure 1C is now Supplementary Figure 2A

Previous Figure 1D is now Supplementary Figure 2B

Previous Figure 2D is now Supplementary Figure 3A

Previous Figure 2E is now Supplementary Figure 3B

Previous Figure 2F is now Figure 2D

Previous Figure 2G is now Figure 2E

Previous Figure 2H is now Figure 2F

Previous Figure 4B is now Supplementary Figure 5C

Previous Figure 4C is now Figure 4B

Previous Figure 4D is now Figure 4C

Previous Figure 4E is now Supplementary Figure 5D

Previous Figure 4F is now Supplementary Figure 5E

Previous Figure 6 is now Supplementary Figure 5C

Previous Figure 7A is now Figure 6A

Previous Figure 7B is now Figure 6B

Previous Figure 7C is now Figure 6C

Previous Figure 7D is now Figure 6D

Previous Supplementary Figure 1C is now Supplementary Figure 2C

Previous Supplementary Figure 2 is now Supplementary Figure 4

Previous Supplementary Figure 3A is now Supplementary Figure 5A

Previous Supplementary Figure 3B is now Supplementary Figure 5B

Previous Supplementary Figure 4A is now Supplementary Figure 6A

Previous Supplementary Figure 4B is now Supplementary Figure 6B

Previous Supplementary Figure 5 is now Supplementary Figure 7

Previous Supplementary Figure 6A is now Supplementary Figure 8A

Previous Supplementary Figure 6B is now Supplementary Figure 8B

Previous Supplementary Figure 6C is now Supplementary Figure 8C

Previous Supplementary Figure 7 is now Figure 7A

Previous Supplementary Figure 8A is now Figure 7B

Previous Supplementary Figure 8B is now Figure 7C

References

Revised AMA format

Word count

Text was trimmed from 14,624 to 11,668 words

Inherited p40^{phox} deficiency differs from classic chronic granulomatous disease

Annemarie van de Geer[1#], Alejandro Nieto-Patlán[2,3,4#], Douglas B. Kuhns[5], Anton T.J. Tool[1], Andrés A. Arias[6,7°], Matthieu Bouaziz[2,3°], Martin de Boer[1°], José Luis Franco[6°], Roel P. Gazendam[1°], John L. van Hamme[1°], Michel van Houdt[1°], Karin van Leeuwen[1°], Paul J.H. Verkuijlen[1°], Timo K. van den Berg[1,8°], Juan F. Alzate[9°], Carlos A. Arango-Franco[6,7°], Vritika Batura[10°], Andrea R. Bernasconi[11°], Barbara Boardman[12°], Claire Booth[13°], Siobhan O. Burns[14,15°], Felipe Cabarcas[16°], Nadine Cerf Bensussan[17,18,19°], Fabienne Charbit-Henrion[17,18,19,20°], Anniek Corveleyn[21°], Caroline Deswarte[2,3°], María Esnaola Azcoiti[2,22°], Dirk Foell[23°], John I. Gallin[24°], Carlos Garcés[6°], Margarida Guedes[25°], Claas H. Hinze[23°], Steven M. Holland[26°], Stephen M. Hughes[12°], Patricio Ibañez[27°], Harry L. Malech[24°], Isabelle Meyts[28,29°], Marcela Moncada-Velez[6°], Kunihiko Moriya[2,3°], Esmeralda Neves[30°], Matias Oleastro[11°], Laura Perez[11°], Vimel Rattina[2,3°], Carmen Oleaga-Quintas[2,3°], Neil Warner[31°], Aleixo M. Muise[31,32°], Jeanet Serafín López[4°], Eunice Trindade[33°], Julia Vasconcelos[30°], Séverine Vermeire[34,35°], Helmut Wittkowski[23°], Austen Worth[13°], Laurent Abel[2,3,36°], Mary C. Dinauer[37°], Peter D. Arkwright[12°], Dirk Roos[1§@], Jean-Laurent Casanova[2,3,38,39§ @], Taco W Kuijpers[1,40,41§@] and Jacinta Bustamante[2,3,42§@]

1. Department of Blood Cell Research, Sanquin Research, Academic Medical Center, University of Amsterdam, Amsterdam, The Netherlands, EU
2. Laboratory of Human Genetics of Infectious Diseases, Necker Branch, INSERM U1163, Necker Hospital for Sick Children, Paris, France, EU
3. Paris Descartes University, Imagine Institute, Paris, France, EU
4. Department of Immunology, National School of Biological Science, National Polytechnic Institute, ENCB - IPN, Mexico, Mexico
5. Neutrophil Monitoring Laboratory, Clinical Services Program, Leidos Biomedical Research, Inc., Frederick National Laboratory for Cancer Research, Frederick, MD, USA
6. Primary Immunodeficiencies Group, Department of Microbiology and Parasitology, School of Medicine, University of Antioquia UdeA, Medellin, Colombia
7. School of Microbiology, University of Antioquia UdeA, Medellin, Colombia
8. Department of Molecular Cell Biology and Immunology, VU Medical Center, VU University, Amsterdam, The Netherlands, EU
9. National Center for Genomic Sequencing-CNSG, University Research Branch - SIU, School of Medicine, University of Antioquia UdeA, Medellin, Colombia
10. Department of Pediatrics and Biochemistry, University of Toronto, Hospital for Sick Children, Toronto, Ontario, Canada
11. Service of Immunology and Rheumatology, Garrahan National Pediatric Hospital, Buenos Aires, Argentina
12. Department of Pediatric Allergy and Immunology, Royal Manchester Children's Hospital, University of Manchester, Manchester, UK, EU
13. Department of Immunology, Great Ormond Street Hospital NHS Foundation Trust, London, UK
14. Institute of Immunity and Transplantation, University College London, London, UK
15. Department of Clinical Immunology, Royal Free London NHS Foundation Trust, London, UK

16. Group of Embedded System and Computational Intelligence -SISTEMIC, Department of Electric Engineering, Engineering Faculty, University of Antioquia UdeA, Medellin, Colombia
17. Laboratory of Intestinal Immunity, INSERM U1163, Imagine Institute, Paris, France, EU
18. GENIUS group (GENetically ImmUne-mediated enteropathieS) from the European Society for Pediatric Gastroenterology, Hepatology and Nutrition (ESPGHAN)
19. Paris Descartes University, Paris, France, EU
20. Pediatric Gastroenterology, Hepatology and Nutrition Unit, AP-HP, Necker Hospital for Sick Children, Paris, France, EU
21. Department of Human Genetics, University Hospitals Leuven, Leuven, Belgium, EU
22. Department of Immunology, Ricardo Gutierrez Children's Hospital, Buenos Aires, Argentina
23. Department of Pediatric Rheumatology and Immunology, Munster University Hospital, Germany, EU
24. Laboratory of Host Defenses, NIAID, NIH, Bethesda, MD, USA
25. Department of Pediatrics, Santo Antonio Hospital, Porto, Portugal, EU
26. Laboratory of Clinical Infectious Diseases, NIAID, NIH, Bethesda, MD, USA
27. Inflammatory Bowel Disease Program, Gastroenterology Department, Clinic Las Condes Medical Center, University of Chile, Santiago de Chile, Chile
28. Department of Pediatric Hematology and Oncology, University Hospitals Leuven, KU Leuven, Leuven, Belgium, EU
29. Department of Microbiology and Immunology, University Hospitals Leuven, KU Leuven, Leuven, Belgium, EU
30. Department of Immunology, Santo Antonio Hospital, Porto, Portugal, EU
31. SickKids Inflammatory Bowel Disease Center and Cell Biology Program, Research Institute, Hospital for Sick Children, Toronto, Ontario, Canada
32. Division of Gastroenterology, Hepatology, and Nutrition, Department of Pediatrics and Biochemistry, University of Toronto, Hospital for Sick Children, Toronto, Ontario, Canada
33. Pediatric Gastroenterology Unit, Sao Joao Hospital, Porto, Portugal, EU
34. Division of Gastroenterology and Hepatology, University Hospitals Leuven, Leuven, Belgium, EU
35. Department of Experimental Medicine, KU Leuven, Leuven, Belgium, EU
36. St Giles Laboratory of Human Genetics of Infectious Diseases, Rockefeller Branch, The Rockefeller University, New York, NY, USA
37. Department of Pediatrics, Washington University School of Medicine, St Louis, MO, USA
38. Howard Hughes Medical Institute, New York, NY, USA
39. Pediatric Hematology and Immunology Unit, AP-HP, Necker Hospital for Sick Children, Paris, France, EU
40. Department of Pediatric Hematology, Immunology & Infectious Diseases, Emma Children's Hospital, Amsterdam, The Netherlands, EU
41. Academic Medical Center, University of Amsterdam, Amsterdam, The Netherlands, EU
42. Center for the Study of Primary Immunodeficiencies, Necker Hospital for Sick Children, AP-HP, Paris, France, EU

#, °, § Equal contributions
@ Corresponding authors

Conflict of interest: The authors have no conflict of interest to declare

Running title: Bi-allelic mutations of *NCF4* underlie p40^{phox} deficiency

Key words: phagocyte, NADPH oxidase, chronic granulomatous disease, infection, hyper-inflammation, *NCF4*

Mailing address:

Dirk Roos
Sanquin Research
Plesmanlaan 125
1066 CX Amsterdam
The Netherlands
Tel. 00-31-20-5123317
E-mail d.roos@sanquin.nl

Jean-Laurent Casanova
The Rockefeller University
1230 York Avenue, New York, NY 10065, USA
Tel. 1-212-327-7331
E-mail jean-laurent.casanova@rockefeller.edu

Taco W Kuijpers
Sanquin Research
PO Box 9190
1006 AD Amsterdam
The Netherlands
Tel. 00-31-20-5123224
E-mail t.w.kuijpers@amc.uva.nl

Jacinta Bustamante
Université Paris Descartes
Institut Imagine, INSERM U-1163
Génétique Humaine des Maladies Infectieuses
24 Boulevard du Montparnasse
75015 Paris, FRANCE, UE
Tel. 33-1-42-75-43-20
E-mail jacinta.bustamante@inserm.fr

Abstract

Bi-allelic loss-of-function mutations of the *NCF4* gene, encoding the p40^{phox} subunit of the phagocyte NADPH oxidase, have been described in only one patient. We report 24 p40^{phox}-deficient patients from 12 additional families in eight countries. These patients display eight different in-frame or out-of-frame mutations of *NCF4*, homozygous in 11 families and compound heterozygous in another. When overexpressed in NB4 neutrophil-like cells and EBV-transformed B cells in vitro, the mutant alleles were found to be loss-of-function, with the exception of the p.R58C and c.120_134del alleles, which were hypomorphic. Particle-induced NADPH oxidase activity was severely impaired in the patients' neutrophils, whereas PMA-induced DHR oxidation, which is widely used as a diagnostic test for CGD, was normal or mildly impaired in the patients. Moreover, the NADPH oxidase activity of EBV-transformed B cells was also severely impaired, whereas that of mononuclear phagocytes was normal. Finally, the killing of *Candida albicans* and *Aspergillus fumigatus* hyphae by neutrophils was conserved in these patients, unlike in CGD patients. The patients suffer from hyper-inflammation and peripheral infections, but they do not display any of the invasive bacterial and fungal infections seen in CGD. Inherited p40^{phox} deficiency underlies a distinctive condition, resembling a mild, atypical form of CGD.

Introduction

Chronic granulomatous disease (CGD) is a recessive primary immunodeficiency (PID) caused by loss-of-function mutations of autosomal or X-linked genes encoding five components of the phagocyte reduced nicotinamide adenine dinucleotide phosphate (NADPH) oxidase complex (1) . This enzyme catalyzes the production of reactive oxygen species (ROS) in phagocytes. CGD was first described in 1954 (2) , the first functional disorder of phagocytes to be identified in 1966 (3), and its first genetic etiology, which is X-linked recessive (XR), was discovered in 1986, in the first positional identification of a PID gene (4, 5). The other genetic etiologies proved to be autosomal recessive (AR) (6). CGD patients suffer from recurrent, life-threatening, invasive infections with specific bacteria and fungi (7-10). Severe parasitic infections have rarely been reported in CGD patients, who also seem to have no particular predisposition to severe viral illnesses (11). Systemic hyper-inflammation, including granulomatous lesions of the respiratory and gastrointestinal (GI) tracts in particular, is also common (12-14). Patients with CGD may initially present with unexplained granulomatosis, which is associated with a poor prognosis, (13, 15). Autoimmune conditions, such as systemic lupus erythematosus, are rare in CGD patients (16). The X-linked recessive (XR, gp91^{phox} [*ph*agocyte *ox*idase]) form of CGD is clinically more severe than the AR p47^{phox} deficient form (7, 9, 17). AR p22^{phox} and p67^{phox} deficiencies appear to be as severe as XR-CGD (18, 19). Patients are routinely placed on prophylactic antimicrobial therapy, and the only curative treatment widely available is allogeneic hematopoietic stem cell transplantation (HSCT) (20).

The NADPH oxidase of human phagocytes is a complex of at least five subunits. The membrane-bound component is a heterodimer consisting of gp91^{phox} and p22^{phox}, encoded by the X-linked *CYBB* gene and the autosomal *CYBA* gene, respectively. This heterodimer is known as flavocytochrome b_{558} and is the catalytic core of the NADPH oxidase complex (21). The second component is a cytosolic heterotrimer composed of p40^{phox}, p47^{phox}, and p67^{phox},

which form the regulatory part of the NADPH oxidase and are encoded by *NCF4*, *NCF1,* and *NCF2,* respectively (22). The membrane-bound and cytosolic components do not interact in steady-state conditions. Upon phagocyte activation, after the phagocytosis of a bacterium or fungus, for example, the two components and a small GTPase (Rac1 and/or Rac2) are activated and assemble on the phagosomal membrane, to produce superoxide (O_2^-) in the phagosome (23). This O_2^- is subsequently converted into hydrogen peroxide (H_2O_2) and other ROS, which together contribute to the destruction of the phagocytized microorganisms. Loss-of-function (LOF) mutations of *CYBB* underlie the XR form of CGD, whereas LOF mutations of *CYBA*, *NCF1*, and *NCF2* underlie AR forms. Hypomorphic mutations of some of these genes have been shown to underlie 'variant CGD', in which residual activity does not differ between cell types (24). Hypomorphic *CYBB* mutations, which are more deleterious in monocyte-derived macrophages (MDMs) than in peripheral phagocytes, have been shown to underlie Mendelian susceptibility to mycobacterial disease (MSMD) (25).

Much less is known about the fifth component, $p40^{phox}$, as bi-allelic mutations of *NCF4* have only ever been described once before, in a young boy with severe colitis (26). $p40^{phox}$ has three domains: PX, PB1, and SH3 (27, 28). During phagocytosis, the upregulation of the membrane phospholipid phosphatidylinositol 3-phosphate [PI(3)P] and subsequent high-affinity binding of the $p40^{phox}$ PX domain enhance NADPH oxidase activity (21, 29). The $p40^{phox}$-deficient patient is compound heterozygous for a premature stop codon and a missense mutation in the PX domain compromising binding to PI(3)P which results in the impairment of neutrophil phagocytosis-induced oxidase activity (26). As in classic CGD neutrophils, intracellular oxidant production after stimulation with serum-opsonized zymosan, IgG-beads, or serum-opsonized *Staphylococcus aureus,* is impair in the patient's neutrophils, and *S. aureus* killing is also defective (20, 26, 30). However, in this patient, unlike classic CGD patients, the

production of O_2^- by neutrophils in response to stimulation with phorbol-myristate acetate (PMA) or formyl-methionyl-leucyl-phenylalanine (fMLF) is normal (26). The killing of *S. aureus* by neutrophils is also impaired in p40^{phox}–deficient and CGD mice (31). However, p40^{phox}-deficient murine neutrophils display highly impaired ROS production upon stimulation with PMA or heat-killed *S. aureus*, but not serum-opsonized zymosan (32). Moreover, gp91^{phox} and p47^{phox} KO mice (33-35) seem to have a less severe form of inflammatory colitis than p40^{phox} KO mice (36, 37). The cellular and clinical overlap and differences between human p40^{phox} deficiency and classic CGD are largely unknown. We describe here the characterization of 24 patients from 12 families in eight countries with bi-allelic mutations of *NCF4*.

Results

Bi-allelic *NCF4* mutations in 24 individuals from 12 families in eight countries

We studied 20 patients from 12 families with clinical features suggestive of CGD (Kindreds A to L) (Table 1, Figure 1A). The families originated from Pakistan (Kindreds A, B, E, and F), Portugal (C and J), Australia (D), Colombia (G), Argentina (H), Kuwait (I), Russia (K) and Chile (L). Whole-exome sequencing (WES) or targeted next-generation sequencing (NGS) with a panel of PID genes identified homozygous variants of the *NCF4* gene in patients from 11 families: two variants affecting essential splice sites (c.118-1G>A in kindreds A, E, and K; and c.32+2T>G in kindred F), three missense variants (c.314G>A in kindred B resulting in p.R105Q; c.172C>T in kindreds G and L resulting in p.R58C; and c.430C>A in kindred H resulting in p.P144T), one nonsense variant (c.716G>A in kindred I resulting in p.W239X) and one in-frame deletion (c.120_134del in kindreds C and J). Finally, we found compound heterozygous splice-site variants in one family (c.118-1G>A and c.759-1G>C, kindred D). All variants were verified by Sanger sequencing. In 11 kindreds, the familial segregation of the alleles was consistent with an AR trait. Kindred J displayed uniparental isodisomy (UPD), as both copies of chromosome 22 were inherited from the father (Figure 1A) (38). Four asymptomatic individuals were shown to carry bi-allelic mutations (Kindreds E and G) (Figure 1A). None of the variants other than p.R58C (MAF=0.001) were found in public databases (Exome Aggregation Consortium, Human Gene Mutation Database, GnomAD, and Bravo database) or in our in-house WES database (~4,500 WES) . Furthermore, combined annotation-dependent depletion (CADD) scores predicted all mutations to be deleterious, as these scores were above or close to the mutation significance cutoff (MSC) (Supplementary Figure 1A) (24). The three missense mutations affect residues located in the PX domain of the $p40^{phox}$ protein (Figure 1B). These residues are highly conserved in other species, suggesting that they

have an important function in the p40^{phox} protein (Supplementary Figure 1B). We searched for a founder effect accounting for the presence of the c.120_134del, c.118-1G>A, and p.R58C mutations in different families. The patients homozygous for these mutations were genotyped with the genome-wide array 6.0. The c.120_134del mutation in two Portuguese families (Kindreds C and J) is within a common haplotype of 884 kb and 1,926 SNPs, demonstrating a founder effect. We dated the most common recent ancestor (MRCA) to 175 years ago: confidence interval: 50-650 years). The c.118-1G>A variant in patients from Pakistan (Kindreds A and E) is within a common haplotype of 337 kb and 136 SNPs. The MRCA of these kindreds was dated to 1,950 years ago (confidence interval 625-8,075 years). The patient from Russia (K) also shared a common haplotype of 152 kb and 41 SNPs in common with the two Pakistani patients, suggesting a common ancestor for these three patients, and the MRCA was estimated to have lived 6,275 years ago (confidence interval 2,475-19,000 years) (39). Finally, the c.172C>T (p.R58C) mutation, present in two Latin American kindreds, is within a common haplotype of 122 kb and 47 SNPs. The MRCA of these kindreds was dated to 4,425 years ago (confidence interval 1,375-16,025 years). Collectively, these data suggest that 24 individuals from 12 kindreds in eight countries suffer from inherited p40^{phox} deficiency, including 20 symptomatic and four asymptomatic individuals (Figure 1A).

Impaired *NCF4* mRNA expression in the patients' cells

We measured *NCF4* transcript levels in cells from the patients and healthy controls, by quantitative real-time RT-PCR (qPCR). Epstein-Barr virus-transformed B-cell lines (EBV-B cells) and neutrophils homozygous for c.32+2T>G (P14) produced no *NCF4* transcripts detectable by qPCR (Supplemental Figure 2A), or cDNA-PCR, (data not shown). These findings suggest that transcripts carrying this mutation are subjected to nonsense-mediated

mRNA decay. For P12 (c.118-1G>A), P15 (p.R58C), P20 (p.W239X) and P22 (c.120_134del), *NCF4* transcript levels in EBV-B cells and neutrophils were lower than those in 10 unrelated controls (Supplemental Figure 2A). Cells homozygous for c.118-1G>A or c.120_134del produced transcripts of lower molecular weight (MW), suggesting the occurrence of alternative splicing. By TOPO-TA cloning, three aberrantly spliced variants were detected for c.118-1G>A, all of which were predicted to encode truncated proteins, and a fourth minor transcript (6%) with a large in-frame deletion, c.118_198del, was identified (Supplemental Figure 2B). For c.120_134del, most of the transcripts carried a five-codon deletion (p.F41_V45del) at the beginning of exon 3; another three aberrantly spliced variants were predicted to encode truncated proteins (Supplemental Figure 2B). Finally, for the c.759-1G>C allele, we performed exon trapping. Three spliced variants were obtained: one with the retention of 37 bp of intron 8a (63%), one in which all of intron 8a was retained (26%), and one with the retention of 16 bp of intron 8a (11%) (Supplementary Figure 2C).

The mutant *NCF4* alleles are deleterious in EBV-B cells

We assessed the potential impact of all individual *NCF4* alleles. We used HEK293T cells for analyses of $p40^{phox}$ protein expression, whereas, for analyses of $p40^{phox}$ function, we used EBV-B cells from patient P14 (homozygous for c.32+2T>G), designated as $NCF4^{-/-}$, as they produced no detectable *NCF4* mRNA. We first evaluated protein expression by transfecting HEK293T cells with expression vectors carrying C-terminally Flag-tagged-WT or mutant *NCF4* cDNAs (R58C, R105Q, P144T, W239X, c.118_198del, and c.120_134del). Immunoblot analyses revealed that the WT, R58C, R105Q, and P144T cDNAs encoded a single full-length 40-kDa protein that was produced in large amounts. By contrast, cells transfected with the in-frame deletions, c.118_198del and c.120_134del, produced proteins

with a lower MW, at much lower abundance. Finally, the protein encoded by W239X cDNA was not detected with an anti-Flag Ab, whereas a truncated protein of about 25 kDa gave a low-intensity signal with an anti-p40^{phox} Ab (Figure 2A). We investigated the mode of functioning of the mutant alleles (LOF or hypomorphic), in EBV-B cells, which express all components of the NADPH oxidase complex and produce ROS (25, 26, 40). We transduced *NCF4*$^{-/-}$ EBV-B cells from patient P14 with retroviruses for the overexpression of missense (R58C, R105Q and P144T), in-frame deletion (c.120_134del) and nonsense (W239X) cDNAs. Western blotting confirmed that the missense proteins were expressed normally, whereas c.120_134del was produced in small amounts and the W239X protein was undetectable (Figure 2B). We then evaluated ROS production in *NCF4*$^{-/-}$ EBV-B cells, by measuring superoxide O_2^- levels after PMA stimulation. EBV-B cells transduced with the R58C, R105Q, P144T, c.118_198del, p.Asp254Serfs96*, and W239X alleles produced no detectable O_2^-. By contrast, retro-transduction with the c.120_134del variant led to a small, reproducible increase in O_2^- production (Figure 2C). No H_2O_2 was generated following the retrovirus-mediated transduction of *NCF4*$^{-/-}$ EBV-B cells with any of the mutant alleles in these conditions (Supplemental Figure 3A). These data suggest that six of the seven alleles tested were LOF, the remaining allele (c.120_134del) being severely hypomorphic, under these experimental conditions at least.

The mutant *NCF4* alleles are deleterious in NB4 cells

We then generated CRISPR-Cas9 knockout p40^{phox} NB4 cells, which we allowed to differentiate into neutrophil-like cells. NADPH oxidase activity and *S. aureus* killing capacities were assessed in NB4-p40^{phox}-KO cells, and in NB4-p40^{phox}-KO cells reconstituted with alleles R105Q, R58C, c.120_134del and c.118_198del or WT-p40^{phox}. No decrease in PMA-induced

extracellular H_2O_2 release or intracellular H_2O_2 generation was observed in NB4-p40^{phox}-KO cells, as with cells reconstituted with any of the mutant alleles, consistent with the results obtained with neutrophils from the previously reported p40^{phox}-deficient patient (Figure 2D and Supplemental Figure 3B) (26). Assessments of extracellular H_2O_2 release in response to serum-opsonized *E. coli* and *A. fumigatus* hyphae showed that NADPH oxidase activity was impaired in NB4-p40^{phox}-KO cells (Supplemental Figure 3B). This defect was restored by reconstitution with WT-p40^{phox} or the R58C allele, but not with the other three mutant alleles (Supplemental Figure 3B). Nevertheless, for *E. coli*-induced intracellular DHR oxidation, only WT-p40^{phox} restored the NADPH oxidase activity (Figure 2E). Moreover, *S. aureus* killing was impaired in NB4-p40^{phox}-KO cells, and in cells reconstituted with any of the mutant alleles, with the exception of the R58C allele (Figure 2F). These experiments suggest that the R105Q, c.120_134del and c.118_198del alleles are LOF in terms of ROS production and *S. aureus* killing in NB4 cells. In contrast, the R58C allele is hypomorphic in the same experimental conditions. Collectively, these data indicate that all the *NCF4* alleles tested are LOF, with the exception of c.120_134del in EBV-B cells and R58C in NB4 cells, at least upon overexpression.

Impaired p40^{phox} expression in the patients' phagocytes

We studied the expression of endogenous p40^{phox} by western blot, in neutrophils, monocytes, MDMs and monocyte-derived dendritic cells (MDDCs). We detected no p40^{phox} protein in neutrophils from P1 (c.118-1G>A), P9 and P10 (c.120_134del), P11 (c.118-1G>A/c.759-1G>C), P12 (c.118-1G>A), P14 (c.32+2T>G), P22 (c.120_134del), and P23 (c.118-1G>A). By contrast, neutrophils from P6 and P8 (R105Q), and from P15 and P16 (R58C), had normal levels of p40^{phox} protein. Neutrophils from P20 (W239X) contained a

lower MW protein present at low abundance (Figure 3A), consistent with the truncated protein observed upon W239X overexpression in HEK293T cells (Figure 2A). Western blotting also revealed that the levels of the other components of the NADPH oxidase complex in the patients' neutrophils were normal (Supplementary Figure 4). Finally, no $p40^{phox}$ protein was detected in MDMs and MDDCs from P12, P20, and P22, (Figure 3B). Thus, these mutations result in a loss of $p40^{phox}$ expression in various types of myeloid cells. Collectively, these data are consistent with those obtained for the overexpression of mutant cDNAs in recipient cells.

Impaired $p40^{phox}$ expression in the patients' EBV-B cells

We studied the expression of the NADPH oxidase subunits by western blotting, with EBV-B cells (26). We observed a complete loss of expression of the $p40^{phox}$ protein in EBV-B cells from P12, P14, P20, and P22. By contrast, $p40^{phox}$ was detected, but at low abundance, in cells from P15 (Figure 3C). The other subunits of the NADPH oxidase complex, $gp91^{phox}$, $p22^{phox}$, and $p47^{phox}$, were normally expressed in the cells of all patients, as shown by western blotting and flow cytometry with intracellular staining (Figure 3C, D) and comparing with $gp91^{phox}$-, $p22^{phox}$-, and $p47^{phox}$-deficient patients. However, the expression of $p67^{phox}$, which interacts with $p40^{phox}$, was affected in the EBV-B cells (Figure 3D), but not the neutrophils (Supplementary Figure 4). These findings indicate that $p40^{phox}$ is involved in stabilizing $p67^{phox}$ levels in EBV-B cells, but not in neutrophils.

Residual-to-normal levels of NADPH oxidase activity in $p40^{phox}$-deficient neutrophils exposed to soluble inducers

We studied the impact of *NCF4* mutations on NAPDH oxidase activity, by evaluating ROS production in patient's cells. The PMA-induced DHR test, which measures intracellular H_2O_2 generation, is widely used on neutrophils for the diagnosis of classic CGD (1). This test

showed a wide range of intracellular ROS production activity in p40^{phox}-deficient neutrophils, from completely normal oxidase activity to residual levels of activity, but always markedly higher than those in classic CGD cells (Figure 4A). A similar pattern was observed at several time points (Supplementary Figure 5A). The release of H_2O_2 and production of O_2^- was evaluated after stimulation with PMA, platelet-activating factor (PAF) plus fMLF or serum-opsonized zymosan (SOZ). We found that H_2O_2 generation by the patients' neutrophils was normal or subnormal, whereas neutrophils from classic CGD patients produced no H_2O_2 or O_2^- (Supplemental Figure 4C). Thus, neutrophils from p40^{phox}-deficient patients had normal or impaired, but not abolished ROS production, as shown by extracellular detection tests, contrasting sharply with the results for neutrophils from classic CGD patients.

Impaired NADPH oxidase activity in p40^{phox}-deficient neutrophils exposed to particulate inducers

As previously reported in p40^{phox} KO mice, ROS production in neutrophils in response to particulate stimuli depends on the recruitment of p40^{phox} protein to the endosomes (31). We therefore evaluated intracellular and extracellular ROS production by the patients' neutrophils, following stimulation with serum-opsonized *S. aureus, E. coli, A. fumigatus* hyphae, or *C. albicans*. Particle-induced intracellular DHR oxidation after neutrophil stimulation with *S. aureus* or *E. coli* was severely impaired in all patients tested, as in neutrophils from classic CGD patients (Figure 4B). By contrast, DHR oxidation in neutrophils stimulated with unopsonized or serum-opsonized *C. albicans* conidia was only partially impaired in the p40^{phox}-deficient patients, whereas a more pronounced defect was observed in the neutrophils of classic CGD patients (Figure 4C). Moreover, extracellular H_2O_2 release by the neutrophils of p40^{phox}-deficient patients in response to *S. aureus, E. coli,* or *A. fumigatus* was only partially impaired (Supplemental Figures 5D). Finally, oxygen consumption was slightly impaired in

the cells of all p40^{phox}-deficient patients tested, after stimulation with either soluble (PMA) or particulate (*E. coli*, SOZ) stimuli (Supplemental Figures 5E). Neutrophils lacking gp91^{phox} had no activity at all. Heterozygous carriers of p40^{phox} deficiency displayed no defects of ROS production (data not shown). These findings confirm that p40^{phox} plays an essential role in the NADPH oxidase activity of neutrophils upon stimulation with bacteria and, to a lesser extent, fungi, suggesting the translocation of at p40^{phox}- to assist in activation of the NADPH oxidase complex in response to these microorganisms.

Normal NADPH oxidase activity in other myeloid cells from the patients

We demonstrated that p40^{phox} expression in some patients was equally impaired in different types of phagocytes (Figure 3). We investigated the effects on NADPH oxidase activity in these cells by evaluating ROS production in monocytes, by assessing PMA-induced DHR oxidation. Monocytes from six patients (P12, P15, P16, P19, P20, and P22) responded similarly to cells from healthy controls (Supplementary Figure 5B). We further investigated the NADPH oxidase activity of MDMs, as previously described (25, 41). MDMs from healthy controls, P12, P20, and P22 had normal or low levels of H_2O_2 after stimulation, depending on the stimulus, whereas MDMs from a classic CGD patient released no H_2O_2 (Figure 5A). Finally, we assessed NADPH oxidase activity in MDDCs, again evaluating H_2O_2 release. MDDCs from the three patients tested (P12, P20, and P22) released normal amounts of H_2O_2, as shown by comparison with MDDCs from healthy controls, and unlike MDDCs from classic CGD patients (Figure 5B). Overall, these data suggest that p40^{phox} is redundant in monocytes, MDMs, and MDDCs, in terms of the NAPDH oxidase activity triggered by PMA. Further experiments, assessing particle-induced ROS production by monocytes, MDMs, and MDDCs, are required to determine the extent of this redundancy.

Impaired NADPH oxidase activity in EBV-B cells from patients

We tested EBV-B cells from the p40^{phox}-deficient patients studied here, classic CGD patients, and the first reported patient with p40^{phox} deficiency (42). In luminol bioluminescence assays, EBV-B cells from P12, P14, P15, and P20 displayed severely impaired NADPH oxidase activity (Figure 5C). By contrast, EBV-B cells from P22 (with c.120_134del) displayed residual luminescence, consistent with the results obtained following the retrovirus-mediated transduction of NCF4$^{-/-}$ EBV-B cells with the c.120_134del allele (Figure 2C). This allele is, therefore, also constitutively hypomorphic. We then evaluated the release of H_2O_2 in EBV-B cells from P12, P14, and P20. H_2O_2 detection was completely negative, as in cells from classic CGD patients. By contrast, EBV-B cells from P22 and P15 displayed a residual release of H_2O_2 (Figure 5C). Finally, EBV-B cells from P12, P14, P15, and P20 were transduced with a p40^{phox} WT cDNA. The rescue of p40^{phox} protein expression was confirmed by immunoblotting before functional assays (Supplementary Figure 6A). O_2^- production$^-$ production in response to PMA stimulation was restored in the transduced EBV-B cells (Supplementary Figure 6B). These experiments with EBV-B cells demonstrate that p40^{phox} is not redundant for NADPH oxidase complex activity in these cells. They also confirm that one of the eight *NCF4* alleles is severely hypomorphic.

Impaired killing of *Staphylococcus,* but not of fungi, by the patients' cells

We then assessed the ability of the patients' neutrophils to kill various microorganisms that commonly cause disease in classic CGD patients. The phagocytosis of serum-opsonized *E. coli, S. aureus, C. albicans,* and zymosan (SOZ) by the patients' neutrophils was similar to that by neutrophils from healthy controls and classic CGD patients (data not shown). Non-

oxidative phagocyte killing involves the release of the proteolytic content of granules into the phagosome or at the neutrophil plasma membrane. In the $p40^{phox}$-deficient neutrophils tested, protease release from the azurophilic granules (elastase, cathepsin G) in the DQ-BSA assay did not differ from that of neutrophils from healthy controls (data not shown) and classic CGD patients (43). We therefore analyzed the phagocyte-mediated killing of different species of bacteria and fungi. The killing of *S. aureus* by the patients' neutrophils was markedly impaired for all the patients tested, similar to that observed for the classic CGD neutrophils.(Figure 6A) (44). *E. coli* killing was unaffected in the patients' neutrophils, as in those of classic CGD patients (Figure 6B) (45). By contrast, the killing of *A. fumigatus* was normal or subnormal, whereas neutrophils from classic CGD patients were completely incapable of killing these hyphae (Figure 6C). *C. albicans* killing by the patients' neutrophils was similar to that by the neutrophils of healthy control cells when *C. albicans* was opsonized, whereas neutrophils from classic CGD patients were unable to kill this fungus (Figure 6D). Moreover, inhibition of the germination and hyphenation of *Candida* conidia was similar for neutrophils from the patients and neutrophils from healthy controls (Supplementary Figure 7). Finally, we evaluated the formation of neutrophil extracellular traps (NETs), a process for which ROS have been shown to be essential (46). NET formation in response to PMA was assessed in three patients from Kindreds A, B and C. Only neutrophils from Kindred B (expressing $p40^{phox}$ protein) produced NETs. No NET production was observed in the other $p40^{phox}$-deficient families tested (without $p40^{phox}$ protein expression) or for $gp91^{phox}$-deficient CGD neutrophils (Supplementary Figure 8). These findings suggest that NET formation is dependent on $p40^{phox}$ expression. Collectively, these data indicate that $p40^{phox}$ –deficient neutrophils have normal fungus-killing capacities, unlike classic CGD neutrophils.

Inflammatory lesions in patients with p40^{phox} deficiency

Deficiency of p40^{phox} is not characterized by the invasive bacterial and fungal infections seen in classic CGD, but mostly by inflammatory manifestations, as well as autoimmunity and peripheral infections (Table 1) (Figure 7A). We identified 20 symptomatic patients, of whom 10 (50%) presented skin inflammation (P1, P2, P3, P5, P6, P7, P8, P11, P19 and P24), with lupus-like cutaneous lesions (P1, P6 and P8), or discoid lupus (P3, P7 and P11). Inflammatory, granulomatous gastrointestinal manifestations were found in 10 patients (50%), and included oral ulcers (P1 and P10), abscesses/granulomas (P1, P2, P3, P4, P5, P6, P7, P8, P9, P10, P11, P23, and P24), periodontitis (P9 and P21), gingivitis or gum inflammation (P9, P10, P20, P21), esophagitis (P21 and P23), gastritis (P20), Crohn-like inflammatory bowel disease (IBD) (P1, P11, P21, P22, P23, P24), and perianal abscesses/fistula (P11, P20, P21 and P24). P24 suffered from chronic and severe IBD requiring immunosuppressive treatment and total colectomy. Some lesions were probably both infectious and inflammatory, as often seen in CGD. Three patients (15.7%) (P12, P14, and P19) reportedly suffered from pulmonary infections, including P12, who was later diagnosed with interstitial lung disease that responded well to systemic steroids rather than antibiotics, suggesting an autoinflammatory component. Antibody evaluations were performed in some patients (n=7) suffering from exacerbated inflammation. P1, P4, P5, P7, P8, and P12 were negative for anti-nuclear antibodies (ANA). By contrast, P14 was positive for ANA and anti-neutrophil cytoplasmic antibodies (ANCA), suggesting autoimmune activity in this patient.

Peripheral but not invasive infections in patients with p40^{phox} deficiency

We investigated the possible infectious causes of pulmonary manifestations in the cohort. No pathogen was identified in P19. Cutaneous infections were reported in eight patients (42%) (P1, P4, P6, P7, P9, P11, P21, and P23), three of whom had at least one proven episode

of *S. aureus* infection (P1, P11 and P23). One patient (P15) presented two episodes of disseminated histoplasmosis, which was successfully treated with antifungal drugs and steroids. Ten patients from six different families were vaccinated against tuberculosis with live Bacillus Calmette–Guérin (BCG) (Table 1). No adverse effects were reported in nine patients, whereas P19 developed local lymphadenitis (BCG-itis). This same patient subsequently suffered from meningitis caused by *Mycobacterium avium.* Interestingly, this patient was also heterozygous for a dominant-negative LOF mutation of *STAT1*, responsible for MSMD (47). Four asymptomatic children, aged 1, 3, 8, and 10 years at diagnosis of p40^{phox} deficiency, were found to have homozygous *NCF4* mutations (P13, P16, P17 and P18), demonstrating incomplete clinical penetrance of the disease, at least until adolescence. In summary, p40^{phox} deficiency conferred a variable phenotype marked by non-invasive peripheral infections, mostly of the skin and lungs, and inflammation, mostly of the gastrointestinal tract (Table 1).

Favorable clinical outcome of p40^{phox}-deficient individuals

Inherited p40^{phox} deficiency differs from classic CGD in terms of cellular phenotype and clinical manifestations, but also in terms of clinical outcome (Supplementary Table 1). Mean age at symptom onset was 6 years (range: 1-17 years), later than reported for symptom onset in most classic CGD patients (Supplementary Table 2). Mean age at diagnosis (for patients with symptoms) was 15.3 years (range: 1-46 years), whereas classic CGD is typically diagnosed before the age of five years (Figure 7B and Supplementary Table 2). All patients included in this study are currently alive, and are between the ages of 1 and 47 years (mean: 15.3 years), whereas a mortality of close to 4% per year has been reported for classic CGD (6)(17), with mortality rates highest during in the first two decades of life. The Kaplan-Meier curves for the survival of the largest classic CGD cohort and this p40^{phox}-deficient cohort differed significantly when comparing XR-CGD and p40^{phox} deficiency (p-value=0.0164;

Mantel-Cox analysis) (Figure 7C and Supplementary Table 2). Antibiotic prophylaxis was prescribed in 14 patients. The treatments administered for hyperinflammation included corticosteroids, azathioprine, methotrexate, infliximab, adalimumab, golimumab, ustekinumab and hydroxychloroquine. Due to the severity of clinical manifestations, four patients underwent allogeneic HSCT (P11, P14, P20 and P21), resulting in the resolution of symptoms in all these patients. Overall, $p40^{phox}$ deficiency is a severe condition, but its clinical outcome is nevertheless better than that of classic CGD.

Discussion

We report the molecular, cellular, and clinical characteristics of 24 patients from 12 families with bi-allelic mutations of the *NCF4* gene, encoding the NADPH oxidase p40^{phox} protein. Deficiency of p40^{phox} is caused by homozygous (23 patients, 11 families) or compound heterozygous (one patient) mutations in families from eight countries. Eight novel alleles of the *NCF4* gene were identified, six of them being completely LOF and causing complete p40^{phox} deficiency in the corresponding patients. Upon overexpression, the allele c.120_134del is hypomorphic in EBV-B cells and the allele R58C is hypomorphic in NB4 cells. However, we detected no clinical difference between the patient bearing these variants and the other patients. We further characterized phagocytic cells from the p40^{phox}–deficient patients and compared them with those of patients with other molecular causes of CGD, to define more clearly the contribution of human p40^{phox} to NADPH oxidase activity. Interestingly, *NCF4* bi-allelic mutations were found to result in a cellular phenotype related to, but clearly different from that of other forms of CGD. In particular, the PMA-induced DHR oxidation test widely used for CGD diagnosis gave normal or just below normal values for patients with inherited p40^{phox} deficiency. Diagnosis of p40^{phox} deficiency can be achieved using serum-opsonized *E. coli* as a stimulus in routine DHR- or Amplex Red-based tests, which must be performed in a diagnostic laboratory with expertise in phagocyte respiratory burst analysis. A genetic approach based on Sanger sequencing or NGS of *NCF4* might also facilitate the diagnosis of p40^{phox} deficiency.

The clinical phenotype of patients with p40^{phox} deficiency is also related to but different from that of patients with classic CGD. The patients in this cohort had peripheral infections (mostly staphylococcal) and hyperinflammation (mostly granulomatous lesions of the gastrointestinal tract and skin). Nevertheless, the frequency of inflammatory lesions is lower than in classic CGD patients (48). A few displayed autoimmunity, but, strikingly, none had the

invasive bacterial and fungal infections commonly seen in patients with classic CGD. (7-9, 18). Consistent with these findings, the clinical outcome of p40^{phox} deficiency is better than that of classic CGD. No deaths were recorded in this cohort of patients aged 1 to 46 years, whereas classic CGD-related mortality may reach 35% in its XR and 15% in its AR forms, in the first three decades of life (10, 17). Moreover, four patients remained asymptomatic at ages of one to 10 years, and age at clinical onset ranged from 1 to 17 years in patients with symptoms. The incomplete clinical penetrance observed at one to 10 years of age also contrasts strongly with observations for classic CGD (7-9, 18). Thus, the healthy siblings of probands should be tested immunologically and genetically. Curative and preventive treatments for CGD are based on prolonged treatment with regimens of antibiotics, antifungal drugs, exogenous IFN-γ, and, increasingly, allogeneic HSCT. Decisions concerning allogeneic HSCT for patients with p40^{phox} deficiency should be made on a case-by-case basis, given the milder overall phenotype and greater variability between patients. Similarly, the immediate initiation of antifungal prophylaxis may not be required, whereas treatment with immunosuppressive agents may be indicated.

One patient with disseminated histoplasmosis (P15) was included in this cohort. However, no patient with CGD has ever been reported to suffer from this fungal disease. This situation is reminiscent of that tuberculosis, which is actually much more common than initially thought in CGD patients living in areas of endemic disease (49). Its pathogenesis has been attributed to defects of NADPH oxidase activity in mononuclear phagocytes (25). The normal NADPH oxidase activity of the p40^{phox}-deficient mononuclear phagocytes tested suggests that histoplasmosis may actually be due to the disruption of NADPH oxidase activity in tissue-resident macrophages and dendritic cells, which were not tested in patients with classic CGD or p40^{phox} deficiency (50). Another patient in this cohort had BCG and *M. avium* diseases (P19). BCG disease has been reported in CGD patients, but no case of *M. avium* complex infection

has rarely been reported in this population. Moreover, these two mycobacterial infections are probably not related to p40^{phox} deficiency in P19, because this patient also carries a dominant-negative *STAT1* mutation responsible for MSMD (47). Finally, one of the patients in our cohort had adenocarcinoma (P20), possibly related to the chronic Crohn's colitis of the patient, although other factors may also be involved.

Other clinical features of the patients can be understood in light of their cellular phenotypes. In vitro *S. aureus* killing by neutrophils from patients with p40^{phox} deficiency or classic CGD was severely impaired, whereas *E. coli* killing by neutrophils from these patients was similar to that by neutrophils from healthy controls. *S. aureus* killing is a ROS-dependent process, whereas *E. coli* killing is relatively ROS-independent (45, 51). The absence of invasive *S. aureus* infections in the p40^{phox}-deficient patients was unexpected and remains unexplained, as both in vitro *S. aureus*-induced oxidase activity and *S. aureus* killing are as severely impaired in these patients as in classic CGD patients, who do suffer from invasive *S. aureus* infections. The almost normal killing of fungi by neutrophils from p40^{phox}-deficient patients, even though the killing of *Candida* and *Aspergillus* is ROS-dependent (52, 53), is of direct clinical relevance and contrasts with the situation in classic CGD patients (54). The lack of invasive fungal infections is highly consistent with the in vitro biochemical findings for phagocytic cells from p40^{phox}-deficient patients. Residual NADPH oxidase activity was generally higher in p40^{phox}-deficient cells than in classic CGD cells, and in vitro fungal killing was largely unaffected. This situation contrasts with that for classic CGD, in which invasive fungal infections are among the most feared and life-threatening complications, despite antimicrobial prophylaxis (10), and for which fungus killing is impaired in vitro. Given the importance of p40^{phox}-PX interactions with PI(3)P in the phagosome for the NADPH oxidase activity elicited by bacteria, the lack of effect on *C. albicans*-induced ROS production and killing is surprising. Normal fungal killing in these patients may also result from the residual

fungus-induced NADPH oxidase activity observed, suggesting a p40^{phox}-independent mechanism for ROS production that is preferentially triggered by fungi. This implies that ROS production would have to exceed a certain threshold for effective fungal killing. Further studies of late phagosome formation in relation to p40^{phox} localization and ROS formation might clarify the differences in *S. aureus* and *C. albicans* killing, which diverge in patients with p40^{phox} deficiency, but not in those with classic CGD.

Interestingly, our studies of monocytes, MDMs, and MDDCs suggest that these cell types are not dependent on p40^{phox} for PMA-induced NADPH oxidase activity. This situation contrasts with that for MSMD-causing gp91^{phox} mutations, which disrupt NADPH oxidase activity in MDMs but not in other phagocytes (neutrophils, monocytes, and MDDCs) (25, 41). The conservation of NADPH oxidase activity may explain the milder infectious phenotype of p40^{phox}-deficient patients than of classic CGD patients, including the absence of invasive bacterial and fungal infections. This feature may be specific to human cells, as p40^{phox} mutant mouse macrophages (either KO or R58A mice) have impaired NADPH oxidase activity on stimulation with a physiological stimulus (36). The PX domain of p40^{phox} is thought to have a high affinity and specificity of binding to phosphatidyl-inositol 3-phospate PI(3)P, a lipid on phagosomal membranes, leading to enhanced NADPH oxidase activity. Further studies are required to evaluate NADPH oxidase activity in phagocytic cells other than neutrophils in patients with p40^{phox} deficiency or classic CGD. In this respect, approaches involving the derivation of different types of phagocytes from induced pluripotent stem cells may be particularly effective (55).

Excessive granulomatous inflammation of the skin and gastrointestinal tract was the most common clinical phenotype observed in this cohort of patients. Systemic lupus-like symptoms are rare in CGD patients (7, 12, 20), and in the p40^{phox}-deficient patients reported here. Enhanced inflammation has also been reported in mice with p40^{phox} deficiency (36, 37,

56). Mouse p40^{phox} has been reported to be required for the expression of glycan structure-modifying enzymes, which may underlie the recruitment of neutrophils to resolve intestinal inflammation and facilitate wound healing (37). Mouse macrophages with p40^{phox} p.R58A/R58A or KO mutations also produce smaller than normal amounts of ROS (36). The excessive inflammation seen in classic CGD and p40^{phox} deficiency indicates that ROS play a role in immune regulation (12, 57). Patients with p40^{phox} deficiency display at least as much inflammation as those with classic CGD, but have higher levels of ROS production. The ROS produced by neutrophils may contribute to the clearance of apoptotic cells or cell debris, and their deficiency may contribute to inflammation in various ways, including aberrant efferocytosis, for example (58-62). Alternatively, the inflammation observed in classic CGD and p40^{phox} deficiency may be due to abnormal ROS production by circulating B cells. This possibility was already suggested in the first report describing a p40^{phox}-deficient patient (42). Our results also suggest that NADPH activity is defective in all p40^{phox}-deficient EBV-B cells tested, confirming that p40^{phox} is not redundant in human B cells. An understanding of the excessive inflammation in patients with classic CGD or p40^{phox} deficiency will require further studies of the respiratory burst in various other cell types, including tissue-resident dendritic cells and macrophages, and in different types of circulating B cells.

Materials and Methods

Cell lines

NB4 cells are from DSMZ, Leibniz, Germany. Catalogue # ACC 207.

HEK293T cells are from ATCC Cat. Number CRL-3216.

Ion Torrent sequencing, WES, copy number variation (CNV) and Sanger

We extracted genomic DNA from blood samples with the iPrep PureLink gDNA Blood Kit and iPrep Instruments from Life Technologies. An AmpliseqTM custom panel (Thermo Fisher Scientific, USA) was used in families A-E, J and K. A targeted NGS panel for PID was used in Kindred I (63) and another for IBD was used in Kindred J (64).

WES was performed with 3 µg of DNA from Kindreds F, G, H and L. Exome capture was performed with the SureSelect Human All Exon 72 Mb kit (Agilent Technologies, USA) as previously described. SNP arrays for CNV or ancestral founder effect were used with the Genome-Wide Human SNP Array 6.0 (Affymetrix, USA) in Kindreds A, C, E, G, J, K and L.

For confirmation of the mutations detected and the analysis of familial segregation for kindred members, we amplified the flanking regions of the variants obtained, including part of the intronic regions for all *NCF4* exons studied. Primers and conditions are detailed described in Supplementary Table 3.

NADPH oxidase functional assays.

The NADPH oxidase activity on neutrophil and NB4 was assessed by measuring extracellular H_2O_2 release with an Amplex™ Red kit (Life Technologies, USA). Cells were stimulated with PMA (100 ng/ml), PAF (1 µM) followed by fMLF (1 µM) (all from Sigma-Aldrich), *E. coli* (OD_{600} 0.1, strain ML-35 in the presence of 2 mM azide), S. *aureus* (OD_{600} 0.1, strain Oxford in the presence of 2 mM azide) or *A. fumigatus* hyphae (clinical isolate). We

used $0.25x10^6$ cells/ml and the experiments were performed as previously described (65). The same method was used for the MDMs, MDDCs and EBV-B cells, except that 400 ng/ml PMA was also added for the cells. The abovementioned reagents, *E. coli*, *S. aureus* and *A. fumigatus* strains were used in all experiments throughout this manuscript. Where indicated, particles were opsonized with 10% (v/v) pooled human serum. MDMs and MDDCs were obtained by differentiation as previously described (25, 41). MDMs were cultured for 16 to 18 hours with purified protein derivatives (PPD, 1 mg/ml, tuberculin PPD Batch RT49, Statens Serum Institute, Denmark) or $5x10^3$ IFN-γ IU/ml (Imukin, Boehringer Ingelheim, Germany) then washed and activated by incubation for 30 minutes with PMA, or left unactivated. MDDCs were treated with LPS (1 µg/ml *Salmonella minnesota*, Sigma Aldrich), alone or immediately before treatment with PMA.

The production of intracellular ROS by neutrophils, monocytes and NB4 was analyzed with dihydrorhodamine-1,2,3 (DHR) (Thermo Fisher Scientific, USA), as previously described (66). We added 0.5 µM DHR in DMSO to $2.5x10^6$ neutrophils. PMA (100 ng/ml), serum-opsonized *E. coli* or *S. aureus* (OD_{600} 0.1 in the presence of 2 mM azide), *C. albicans* (OD_{625} 0.1, strain SC5314) or serum-opsonized zymosan (0.1 mg/ml) was then added. At the desired time points, samples were added to STOP-buffer (0.5% (w/v) PFA, 1% (w/v) BSA and 20 mM NaF in PBS), the amount of rhodamine-1,2,3 (mean MFI) was assessed by flow cytometry (FACSCANTO II/LSR) and expressed as the percentage of the rhodamine-1,2,3 produced by healthy control cells.

ROS production by monocytes was analyzed by assessing DHR after stimulation with PMA (400 ng/ml) in Kindreds E, F, G, H and J, with a Galios FACS analyzer (Beckman Coulter, USA) and an LSR Fortessa Cell Analyzer (Becton Dickinson, USA). Where indicated DHR is expressed as a % of control, and MFI values are normalized against the healthy control.

Generation of NB4 p40^{phox} KO cells

The Optimized CRISP Design tool (http://crispr.mit.edu/) was used (Zhang laboratory) to determine the Cas9 target sites present in the coding sequence of p40^{phox}. A oligomer was cloned into the *Bsm*BI site of pLentiCRISPR v2. The constructs were grown in *E. coli Stb*l3. Lentiviral particles were generated by the transient cotransfection of HEK293T cells with pLentiCRISPRv2 – p40^{phox} KO, psPAX2 and pCMV-VSVg, with TransIT-LT1 (Mirusbio). The day after transfection, the cells were plated on NB4 medium. The virus-containing supernatant was harvested on days 2 and 3 after transfection, filtered through 0.45-µm pores, and 1 ml was used with 5x10^5 NB4 cells on two successive days. Transduced NB4 cells were selected with 1 µg/ml puromycin (Invivogen, USA). Surviving cells were plated on limiting dilution medium in a 96-well plate at a density of 0.5 cells/150µl, and growing clones were routinely maintained. The p40^{phox} levels of these clones were assessed by western blotting A clone with no p40^{phox} expression was obtained when the 5´gtcagcaatgttggccgaga 3' target sequence was used.

Statistics

Statistical analysis was performed with GraphPad Prism version 7.02 for Windows (La Jolla, CA, USA). All datasets were considered to be not- normally distributed, as numbers were too low for normality tests. A 2-tailed Mann U Whitney test was used for the statistical analysis, at all times 2 groups were compared: e.g. controls vs. Kindred A, controls vs. Kindred B, etcetera. Data were considered significant when $p<0.05$. For datasets containing multiple independent variables, the Bonferroni correction for multiple testing was applied adjusting the p value dependent on the amount of variables. When $N\geq3$, error bars were added to the graph. When error bars seem to lack in case of $N\geq3$, this is caused by the fact that the SEM is so small that the bars are shorter than the height of the symbol.

Study approval

The study was approved by the institutional review boards of INSERM, Paris, France; Rockefeller University, New York, USA; Necker Hospital for Sick Children, Paris, France, Medical Ethics Committee of the Academic Medical Center/Emma's Children's Hospital, Amsterdam, The Netherlands and by the bioethics committee for research in humans (CBE-SIU) at the University of Antioquia, Medellin, Colombia. All these procedures were conducted in accordance with the 1975 Declaration of Helsinki, as revised in 2013.

Author contributions

T.W.K. and J.B. are the principal investigators; they conceived the study. A.v.d.G, A.N.P., D.B.K., A.T.J.T, P.J.H.V., A.A.A, L.P., M.v.H., M.G., C.O-Q, C.A.A.F., M.E.A., N. W., C.D. and E.N. performed the experiments. D.R., D.B.K., J.I.G., J.L.C M.C.D. and T.K.v.d.B. contributed to the design of the study. A.B., S.B., J.V., S.M.H., E.T., B.B., M.O., M.M.V., S.V., I.M. J.L.F., J.S.L., A.C., F.C.H., P.I., A.M.M., N.C.B., P.D.A, A.W., C.B., D.F, C.H., H.W., S.M.H. and H.M. contributed to collect the samples from the patients and provided a clinical overview. M.d.B, K.v.L., J.F.A, F.C., V.R., V.B., M.B. and L.A. were responsible for genetic analysis. All authors revised the manuscript, and approved the final manuscript. A.v.d.G., A.N.P., D.R., J.L.C., J.B. and T.W.K analyzed the results and wrote the manuscript.

Acknowledgments

The authors thank all patients, their relatives and the treatment teams for their participation in this study. We also thank Céline Desvallées, Dominick Papandrea, Cécile Patissier and Yelena Nemirovskaya for administrative assistance. We thank all the members of the Blood Cell Research Department and the HGMI Laboratory for helpful discussions. We acknowledge the use of the biological resources of the Imagine Institute DNA-biobank (BB-33-00065). A.v.d.G. was supported by Sanquin Blood Supply Product and Process Development Cellular Products Fund (PPOC 1957). A.N.P. was supported by CONACYT National PhD Fellowship Program. The HGMI laboratory was funded in part by the National Institute of Allergy and Infectious Diseases (5R01AI089970 and 5R37AI095983), the National Center for Research Resources and the National Center for Advancing Sciences of the National Institutes of Health (8UL1TR000043), The Rockefeller University, the St. Giles Foundation, *Institut National de la Santé et de la Recherche Médicale* (INSERM), Paris Descartes University, the Integrative Biology of Emerging Infectious Diseases Laboratory of Excellence

(ANR-10-LABX-62-IBEID) and the French National Research Agency (ANR) under the "Investments for the future" program (ANR-10IAHU-01), ANR-IFNPHOX/ANR-13-ISV3-0001-01 and ANR-GENMSMD/ANR-16-CE17-0005-01 (to J.B.), ECOSNord-C14S01 (to J.B. and J.L.F.) and COLCIENCIAS (576-2013 :111556934990 to J.L.F.). K.M. was supported by a Japan Foundation for Pediatric Research fellowship grant. A.M.M. is funded by the CIHR and The Leona M. and Harry B. Helmsley Charitable Trust. This work was supported in part by the Division of Intramural Research, National Institute of Allergy and Infectious Diseases, National Institutes of Health and has been funded in part with federal funds from the National Cancer Institute, National Institutes of Health (HHSN261200800001E). The content of this publication does not necessarily reflect the views or policies of the Department of Health and Human Services, nor does mention of trade names, commercial products, or organizations imply endorsement by the US Government.

References

1. Roos D, Tool ATJ, van Leeuwen K, de Boer M. Biochemical and Genetic Diagnosis of chronic granulomatous disease. In: Seger RA, Roos D, Segal BH, Kuijpers TW, eds. *Chronic granulomatous disease. Geneticcs, Biology and Clinical management*. New York, New York, USA: Nova biomedical Press; 2017:231-300.
2. Janeway CA, Craig, J., Davidson, M., Downey, W., Gitlin, D., Sullivan, J. C. Hypergammaglobulinemia associated with severe recurrent and chronic nonspecific infection. *Am J Dis Child.* 1954 (88):388-392.
3. Holmes B, Quie PG, Windhorst DB, Good RA. Fatal granulomatous disease of childhood. An inborn abnormality of phagocytic function. *Lancet.* 1966;1(7449):1225-1228.
4. Royer-Pokora B, et al. Cloning the gene for an inherited human disorder--chronic granulomatous disease--on the basis of its chromosomal location. *Nature.* 1986;322(6074):32-38.
5. Dinauer MC, Orkin SH, Brown R, Jesaitis AJ, Parkos CA. The glycoprotein encoded by the X-linked chronic granulomatous disease locus is a component of the neutrophil cytochrome b complex. *Nature.* 1987;327(6124):717-720.
6. Segal AW, et al. Absence of cytochrome b-245 in chronic granulomatous disease. A multicenter European evaluation of its incidence and relevance. *N Engl J Med.* 1983;308(5):245-251.
7. Winkelstein JA, et al. Chronic granulomatous disease. Report on a national registry of 368 patients. *Medicine (Baltimore).* 2000;79(3):155-169.
8. Borges de Oliveira-Junior E, et al. Clinical and Genotypic Spectrum of Chronic Granulomatous Disease in 71 Latin American Patients: First Report from the LASID Registry. *Pediatr Blood Cancer.* 2015;62(12):2101-2107.
9. Van den Berg JM, et al. Chronic granulomatous disease: the European experience. *PLoS One.* 2009;4(4):e5234.
10. Marciano BE, et al. Common severe infections in chronic granulomatous disease. *Clin Infect Dis.* 2015;60(8):1176-1183.
11. Parvaneh N, et al. Visceral leishmaniasis in two patients with IL-12p40 and IL-12Rbeta1 deficiencies. *Pediatr Blood Cancer.* 2017;64(6):e26362
12. Magnani A, et al. Inflammatory manifestations in a single-center cohort of patients with chronic granulomatous disease. *J Allergy Clin Immunol.* 2014;134(3):655-662 e658.
13. Marciano BE, Segal BH, Holland SM. Inflammatory Manifestations in Chronic Granulomatous Disease. In: Seger RA, Roos D, Segal H, Kuijpers TW, eds. *Chronic granulomatous disease. Geneticcs, Biology and Clinical management*. New York, New York, USA: Nova biomedical Press; 2017:163-201.
14. Huang C, et al. Genetic Risk for Inflammatory Bowel Disease Is a Determinant of Crohn's Disease Development in Chronic Granulomatous Disease. *Inflamm Bowel Dis.* 2016;22(12):2794-2801.
15. van de Veerdonk FL, Dinauer MC. Dysfunctional processes regulating IL-1B in Chronic Granulomatous Disease. In: Seger RA, Roos D, Segal H, Kuijpers TW, eds. *Chronic granulomatous disease. Geneticcs, Biology and Clinical management*. New York, New York, USA: Nova biomedical Press; 2017:69-87.
16. Ben Abdallah Chabchoub R, Turki H, Mahfoudh A. Systemic lupus erythematosus in a boy with chronic granulomatous disease: case report and review of the literature. *Arch Pediatr.* 2014;21(12):1364-1366.

17. Kuhns DB, et al. Residual NADPH oxidase and survival in chronic granulomatous disease. *N Engl J Med.* 2010;363(27):2600-2610.
18. Wolach B, et al. Chronic granulomatous disease: Clinical, functional, molecular, and genetic studies. The Israeli experience with 84 patients. *Am. J. Hematol.* 2017;92:28-36.
19. Koker MY, et al. Clinical, functional, and genetic characterization of chronic granulomatous disease in 89 Turkish patients. *J Allergy Clin Immunol.* 2013;132(5):1156-1163.
20. Kang EM, Marciano BE, DeRavin S, Zarember KA, Holland SM, Malech HL. Chronic granulomatous disease: overview and hematopoietic stem cell transplantation. *J Allergy Clin Immunol.* 2011;127(6):1319-1326.
21. Segal BH, Leto TL, Gallin JI, Malech HL, Holland SM. Genetic, biochemical, and clinical features of chronic granulomatous disease. *Medicine (Baltimore).* 2000;79(3):170-200.
22. Roos D. Chronic granulomatous disease. *Br Med Bull.* 2016;118(1):50-63.
23. Roos D, de Boer M. Molecular diagnosis of chronic granulomatous disease. *Clin Exp Immunol.*2014;175(2):139-149.
24. Roos D, et al. Two CGD Families with a Hypomorphic Mutation in the Activation Domain of p67phox. *J Clin Cell Immunol.* 2014;5(3).
25. Bustamante J, et al. Germline CYBB mutations that selectively affect macrophages in kindreds with X-linked predisposition to tuberculous mycobacterial disease. *Nat Immunol.*2011;12(3):213-221.
26. Matute JD, et al. A new genetic subgroup of chronic granulomatous disease with autosomal recessive mutations in p40 phox and selective defects in neutrophil NADPH oxidase activity. *Blood.* 2009;114(15):3309-3315.
27. Zhan S, et al. Genomic structure, chromosomal localization, start of transcription, and tissue expression of the human p40-phox, a new component of the nicotinamide adenine dinucleotide phosphate-oxidase complex. *Blood.* 1996;88(7):2714-2721.
28. Matute JD, Arias AA, Dinauer MC, Patino PJ. p40phox: the last NADPH oxidase subunit. *Blood Cells Mol Dis.* 2005;35(2):291-302.
29. Nunes P, Demaurex N, Dinauer MC. Regulation of the NADPH oxidase and associated ion fluxes during phagocytosis. *Traffic.* 2013;14(11):1118-1131.
30. Odell EW, Segal AW. Killing of pathogens associated with chronic granulomatous disease by the non-oxidative microbicidal mechanisms of human neutrophils. *J Med Microbiol.* 1991;34(3):129-135.
31. Ellson CD, Davidson K, Ferguson GJ, O'Connor R, Stephens LR, Hawkins PT. Neutrophils from p40phox-/- mice exhibit severe defects in NADPH oxidase regulation and oxidant-dependent bacterial killing. *J Exp Med.* 2006;203(8):1927-1937.
32. Bagaitkar J, Matute JD, Austin A, Arias AA, Dinauer MC. Activation of neutrophil respiratory burst by fungal particles requires phosphatidylinositol 3-phosphate binding to p40phox in humans but not in mice. *Blood.* 2012;120(16):3385-3387.
33. Deffert C, et al. Hyperinflammation of chronic granulomatous disease is abolished by NOX2 reconstitution in macrophages and dendritic cells. *J Pathol.* 2012;228(3):341-350.
34. Rodrigues-Sousa T, et al. Deficient production of reactive oxygen species leads to severe chronic DSS-induced colitis in Ncf1/p47phox-mutant mice. *PLoS One.* 2014;9(5):e97532.
35. Bao S, Carr ED, Xu YH, Hunt NH. Gp91(phox) contributes to the development of experimental inflammatory bowel disease. *Immunol Cell Biol.* 2011;89(8):853-860.

36. Bagaitkar J, et al. PI(3)P-p40phox binding regulates NADPH oxidase activation in mouse macrophages and magnitude of inflammatory responses in vivo. *J Leukoc Biol.* 2017;101(2):449-457.
37. Conway KL, et al. p40phox expression regulates neutrophil recruitment and function during the resolution phase of intestinal inflammation. *J Immunol.* 2012;189(7):3631-3640.
38. Prando C, et al. Paternal uniparental isodisomy of chromosome 6 causing a complex syndrome including complete IFN-gamma receptor 1 deficiency. *Am J Med Genet A.* 2010;152A(3):622-629.
39. Genin E, Tullio-Pelet A, Begeot F, Lyonnet S, Abel L. Estimating the age of rare disease mutations: the example of Triple-A syndrome. *J Med Genet.* 2004;41(6):445-449.
40. Dusi S, et al. Nicotinamide-adenine dinucleotide phosphate oxidase assembly and activation in EBV-transformed B lymphoblastoid cell lines of normal and chronic granulomatous disease patients. *J Immunol.* 1998;161(9):4968-4974.
41. Conti F, et al. Phagocyte nicotinamide adenine dinucleotide phosphate oxidase activity in patients with inherited IFN-gammaR1 or IFN-gammaR2 deficiency. *J Allergy Clin Immunol.* 2015;135(5):1393-1395.
42. Crotzer VL, et al. Cutting edge: NADPH oxidase modulates MHC class II antigen presentation by B cells. *J Immunol.* 15 2012;189(8):3800-3804.
43. Voetman AA, Weening RS, Hamers MN, Meerhof LJ, Bot AA, Roos D. Phagocytosing human neutrophils inactivate their own granular enzymes. *J Clin Invest.* 1981;67(5):1541-1549.
44. Repine JE, Clawson CC. Quantitative measurement of the bactericidal capability of neutrophils from patients and carriers of chronic granulomatous disease. *J Lab Clin Med.* 977;90(3):522-528.
45. Rosen H, Michel BR. Redundant contribution of myeloperoxidase-dependent systems to neutrophil-mediated killing of Escherichia coli. *Infect Immun.* 1997;65(10):4173-4178.
46. Fuchs TA, et al. Novel cell death program leads to neutrophil extracellular traps. *J Cell Biol.* 2007;176(2):231-241.
47. Kagawa R, et al. Alanine-scanning mutagenesis of human signal transducer and activator of transcription 1 to estimate loss- or gain-of-function variants. *J Allergy Clin Immunol.* 2017;140(1):232-241.
48. Khangura SK, et al. Gastrointestinal Features of Chronic Granulomatous Disease Found During Endoscopy. *Clinical Gastroenterology and Hepatology.* 2016;14(3):395–402.
49. Conti F, et al. Mycobacterial disease in patients with chronic granulomatous disease: A retrospective analysis of 71 cases. *J Allergy Clin Immunol.* 2016;138(1):241-248 e243.
50. Subramanian Vignesh K, Landero Figueroa JA, Porollo A, Caruso JA, Deepe GS, Jr. Granulocyte macrophage-colony stimulating factor induced Zn sequestration enhances macrophage superoxide and limits intracellular pathogen survival. *Immunity.* 2013;39(4):697-710.
51. Zhao XW, et al. Defects in neutrophil granule mobilization and bactericidal activity in familial hemophagocytic lymphohistiocytosis type 5 (FHL-5) syndrome caused by STXBP2/Munc18-2 mutations. *Blood.* 2013;122(1):109-111.

52. Gazendam RP, et al. Human Neutrophils Use Different Mechanisms To Kill Aspergillus fumigatus Conidia and Hyphae: Evidence from Phagocyte Defects. *J Immunol.* 2016;196(3):1272-1283.
53. Boyle KB, Stephens LR, Hawkins PT. Activation of the neutrophil NADPH oxidase by Aspergillus fumigatus. *Ann N Y Acad Sci.* 2012;1273:68-73.
54. Lehrer RI, Cline MJ. Interaction of Candida albicans with human leukocytes and serum. *J Bacteriol.* 1969;98(3):996-1004.
55. Hetzel M, et al. Hematopoietic stem cell gene therapy for IFNgammaR1 deficiency protects mice from mycobacterial infections. *Blood.* 2018;1;131(5):533-545.
56. Winter S, Hultqvist Hopkins M, Laulund F, Holmdahl R. A Reduction in Intracellular Reactive Oxygen Species Due to a Mutation in NCF4 Promotes Autoimmune Arthritis in Mice. *Antioxid Redox Signal.* 2016;25(18):983-996.
57. De Ravin SS, et al. Chronic granulomatous disease as a risk factor for autoimmune disease. *J Allergy Clin Immunol.* 2008;122(6):1097-1103.
58. Fernandez-Boyanapalli RF, et al. Impaired apoptotic cell clearance in CGD due to altered macrophage programming is reversed by phosphatidylserine-dependent production of IL-4. *Blood.* 2009;113(9):2047-2055.
59. Greenlee-Wacker MC, Rigby KM, Kobayashi SD, Porter AR, DeLeo FR, Nauseef WM. Phagocytosis of Staphylococcus aureus by human neutrophils prevents macrophage efferocytosis and induces programmed necrosis. *J Immunol.* 2014;192(10):4709-4717.
60. Greenlee-Wacker MC, Nauseef WM. IFN-gamma targets macrophage-mediated immune responses toward Staphylococcus aureus. *J Leukoc Biol.* 2017;101(3):751-758.
61. Fernandez-Boyanapalli R, et al. Impaired phagocytosis of apoptotic cells by macrophages in chronic granulomatous disease is reversed by IFN-gamma in a nitric oxide-dependent manner. *J Immunol.* 2010;185(7):4030-4041.
62. Marks DJ, Miyagi K, Rahman FZ, Novelli M, Bloom SL, Segal AW. Inflammatory bowel disease in CGD reproduces the clinicopathological features of Crohn's disease. *Am J Gastroenterol.* 2009;104(1):117-124.
63. Frans G, et al. PID in Disguise: Molecular Diagnosis of IRAK-4 Deficiency in an Adult Previously Misdiagnosed With Autosomal Dominant Hyper IgE Syndrome. *J Clin Immunol.* 2015;35(8):739-744.
64. Charbit-Henrion F, et al. Diagnostic Yield of Next-Generation Sequencing in Very Early-Onset Inflammatory Bowel Diseases: A Multicenter Study. *J Crohns Colitis.* In press.
65. Kuijpers TW, Alders M, Tool AT, Mellink C, Roos D, Hennekam RC. Hematologic abnormalities in Shwachman Diamond syndrome: lack of genotype-phenotype relationship. *Blood.* 2005;106(1):356-361.
66. van Pelt LJ, van Zwieten R, Weening RS, Roos D, Verhoeven AJ, Bolscher BG. Limitations on the use of dihydrorhodamine 123 for flow cytometric analysis of the neutrophil respiratory burst. *J Immunol Methods.* 1996;191(2):187-196.

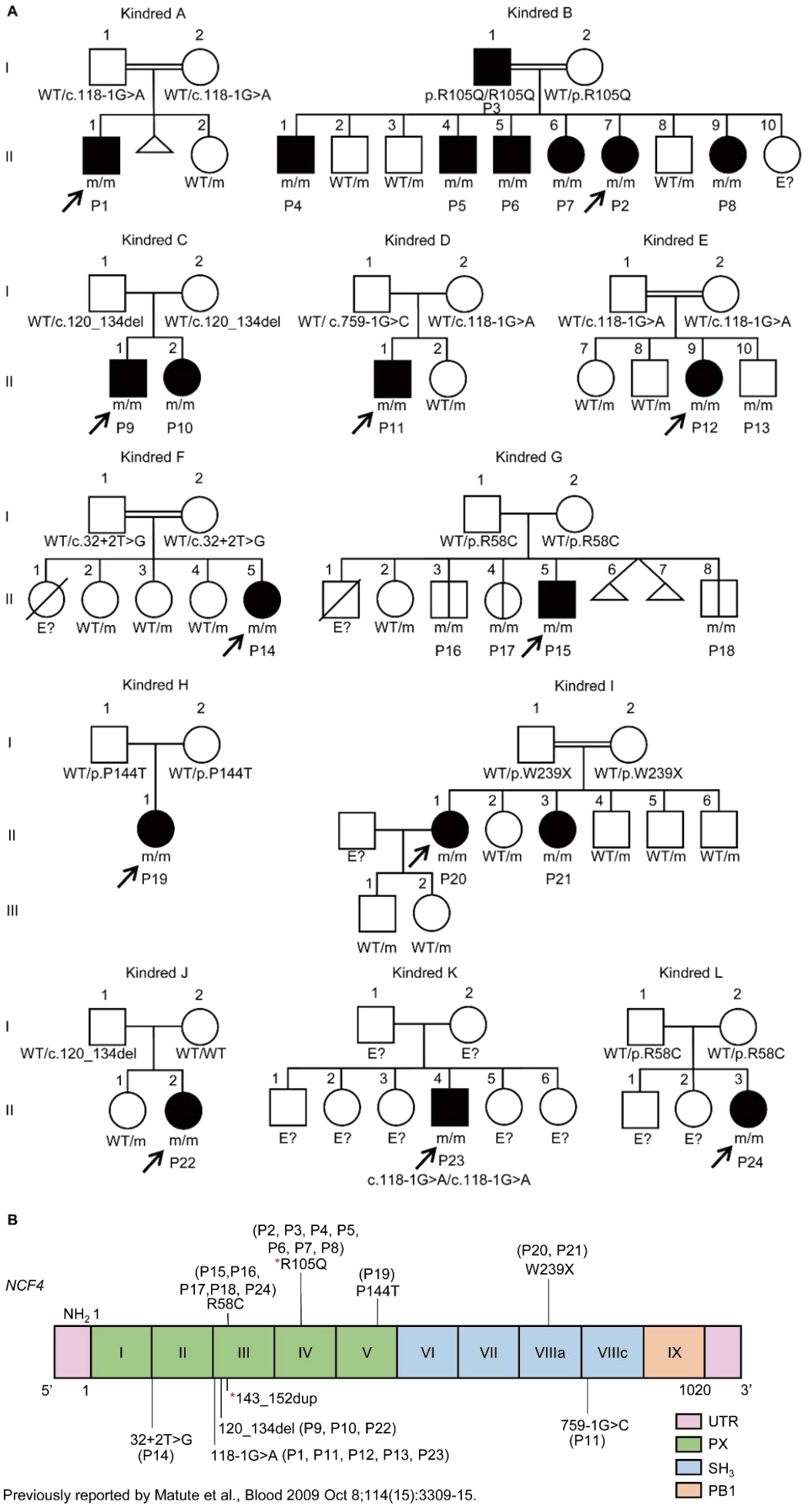
A
Kindred A
WT/c.118-1G>A
WT/c.118-1G>A
m/m
P1
WT/m
Kindred B
p.R105Q/R105Q
WT/p.R105Q
P3
m/m
P4
WT/m
WT/m
m/m
P5
m/m
P6
m/m
P7
m/m
P2
WT/m
m/m
P8
E?
Kindred C
WT/c.120_134del
WT/c.120_134del
m/m
P9
m/m
P10
Kindred D
WT/ c.759-1G>C
WT/c.118-1G>A
m/m
P11
WT/m
Kindred E
WT/c.118-1G>A
WT/c.118-1G>A
WT/m
WT/m
m/m
P12
m/m
P13
Kindred F
WT/c.32+2T>G
WT/c.32+2T>G
E?
WT/m
WT/m
WT/m
m/m
P14
Kindred G
WT/p.R58C
WT/p.R58C
E?
WT/m
m/m
P16
m/m
P17
m/m
P15
m/m
P18
Kindred H
WT/p.P144T
WT/p.P144T
m/m
P19
Kindred I
WT/p.W239X
WT/p.W239X
E?
m/m
P20
WT/m
m/m
P21
WT/m
WT/m
WT/m
WT/m
WT/m
Kindred J
WT/c.120_134del
WT/WT
WT/m
m/m
P22
Kindred K
E?
E?
E?
E?
E?
E?
E?
m/m
P23
c.118-1G>A/c.118-1G>A
Kindred L
WT/p.R58C
WT/p.R58C
E?
E?
m/m
P24
B
NCF4
NH2 1
(P2, P3, P4, P5, P6, P7, P8)
*R105Q
(P15,P16, P17,P18, P24)
R58C
(P19)
P144T
(P20, P21)
W239X
I
II
III
IV
V
VI
VII
VIIIa
VIIIc
IX
5'
1
1020
3'
*143_152dup
32+2T>G
(P14)
120_134del (P9, P10, P22)
118-1G>A (P1, P11, P12, P13, P23)
759-1G>C
(P11)
UTR
PX
SH3
PB1
* Previously reported by Matute et al., Blood 2009 Oct 8;114(15):3309-15.

Figure 1

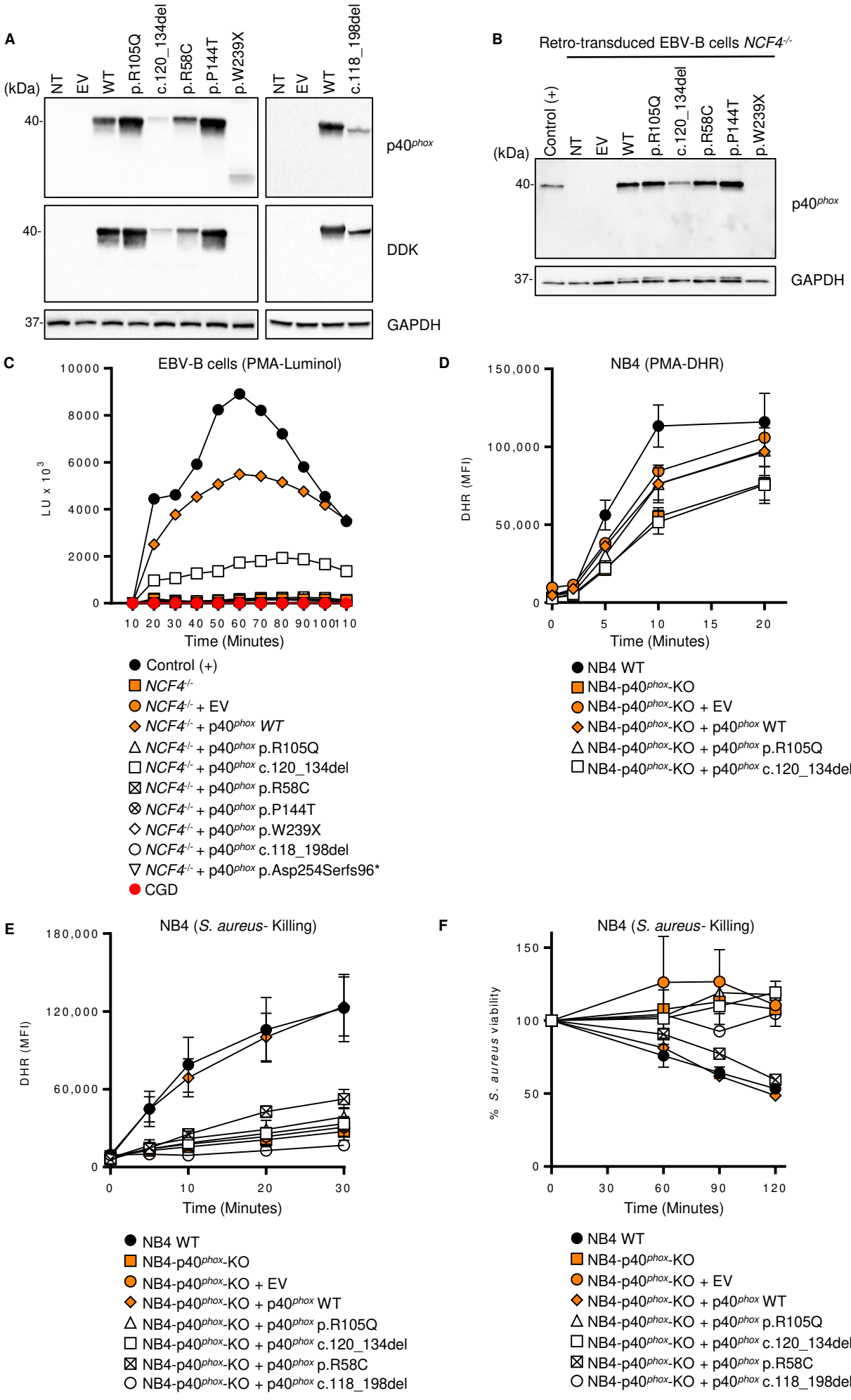
A
(kDa)
NT
EV
WT
p.R105Q
c.120_134del
p.R58C
p.P144T
p.W239X
NT
EV
WT
c.118_198del
40-
40-
37-
p40phox
DDK
GAPDH
B
Retro-transduced EBV-B cells NCF4-/-
Control (+)
NT
EV
WT
p.R105Q
c.120_134del
p.R58C
p.P144T
p.W239X
(kDa)
40-
37-
p40phox
GAPDH
C
EBV-B cells (PMA-Luminol)
LU x 10^3
Time (Minutes)
Control (+)
NCF4-/-
NCF4-/- + EV
NCF4-/- + p40phox WT
NCF4-/- + p40phox p.R105Q
NCF4-/- + p40phox c.120_134del
NCF4-/- + p40phox p.R58C
NCF4-/- + p40phox p.P144T
NCF4-/- + p40phox p.W239X
NCF4-/- + p40phox c.118_198del
NCF4-/- + p40phox p.Asp254Serfs96*
CGD
D
NB4 (PMA-DHR)
DHR (MFI)
Time (Minutes)
NB4 WT
NB4-p40phox-KO
NB4-p40phox-KO + EV
NB4-p40phox-KO + p40phox WT
NB4-p40phox-KO + p40phox p.R105Q
NB4-p40phox-KO + p40phox c.120_134del
E
NB4 (S. aureus- Killing)
DHR (MFI)
Time (Minutes)
NB4 WT
NB4-p40phox-KO
NB4-p40phox-KO + EV
NB4-p40phox-KO + p40phox WT
NB4-p40phox-KO + p40phox p.R105Q
NB4-p40phox-KO + p40phox c.120_134del
NB4-p40phox-KO + p40phox p.R58C
NB4-p40phox-KO + p40phox c.118_198del
F
NB4 (S. aureus- Killing)
% S. aureus viability
Time (Minutes)
NB4 WT
NB4-p40phox-KO
NB4-p40phox-KO + EV
NB4-p40phox-KO + p40phox WT
NB4-p40phox-KO + p40phox p.R105Q
NB4-p40phox-KO + p40phox c.120_134del
NB4-p40phox-KO + p40phox p.R58C
NB4-p40phox-KO + p40phox c.118_198del

Figure 2

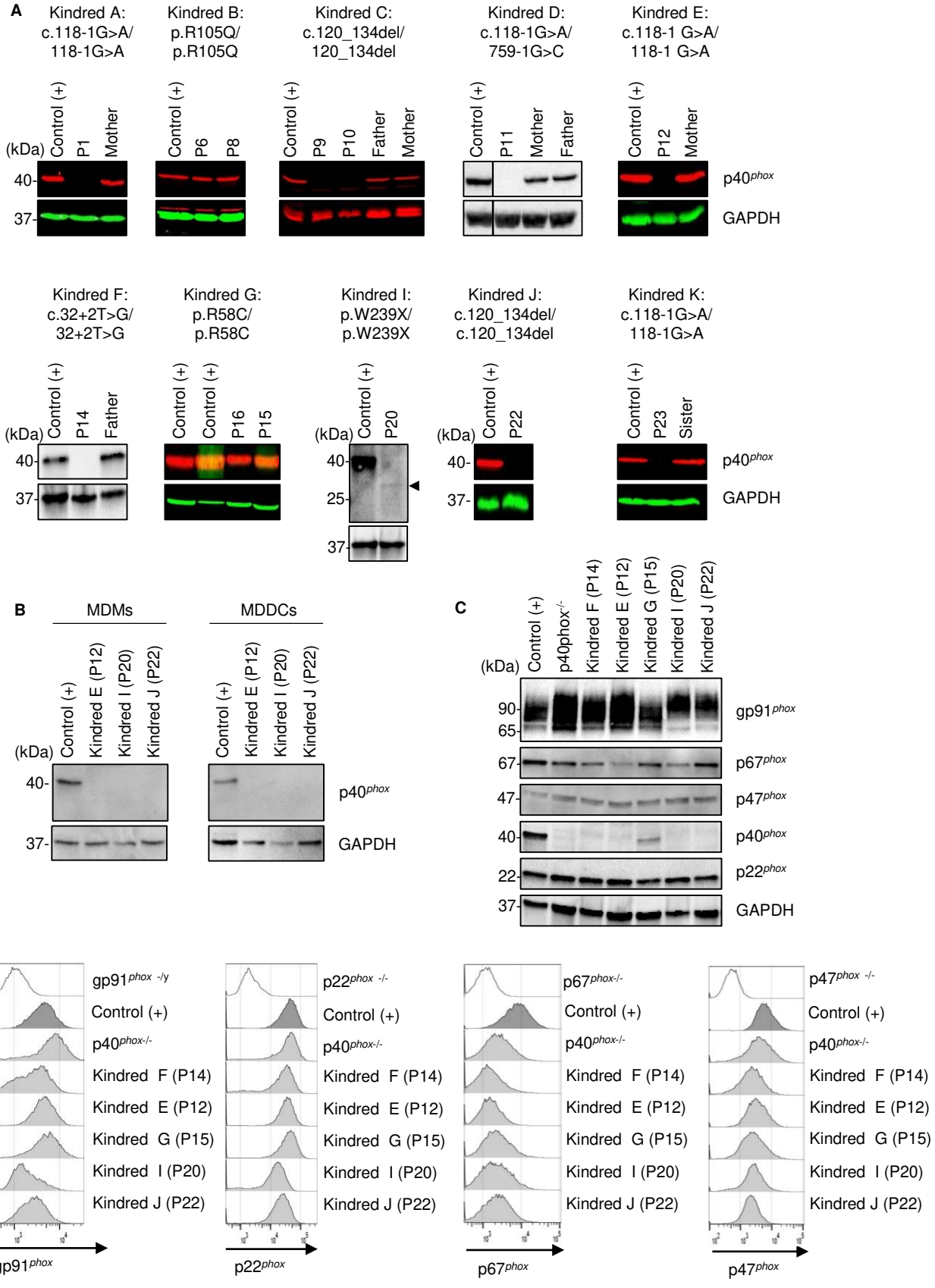
A
Kindred A: c.118-1G>A/ 118-1G>A
Kindred B: p.R105Q/ p.R105Q
Kindred C: c.120_134del/ 120_134del
Kindred D: c.118-1G>A/ 759-1G>C
Kindred E: c.118-1 G>A/ 118-1 G>A
Control (+)
P1
Mother
P6
P8
P9
P10
Father
P11
P12
(kDa)
40-
37-
p40phox
GAPDH
Kindred F: c.32+2T>G/ 32+2T>G
Kindred G: p.R58C/ p.R58C
Kindred I: p.W239X/ p.W239X
Kindred J: c.120_134del/ c.120_134del
Kindred K: c.118-1G>A/ 118-1G>A
P14
Father
P16
P15
P20
25-
P22
P23
Sister
B
MDMs
MDDCs
Kindred E (P12)
Kindred I (P20)
Kindred J (P22)
C
p40phox-/-
Kindred F (P14)
Kindred G (P15)
90-
65-
67-
47-
22-
gp91phox
p67phox
p47phox
p22phox
D
Number of Cells
gp91phox -/y
p22phox -/-
p67phox-/-
p47phox -/-
p40phox-/-
Kindred F (P14)
Kindred E (P12)
Kindred G (P15)
Kindred I (P20)
Kindred J (P22)
gp91phox
p22phox
p67phox
p47phox

Figure 3

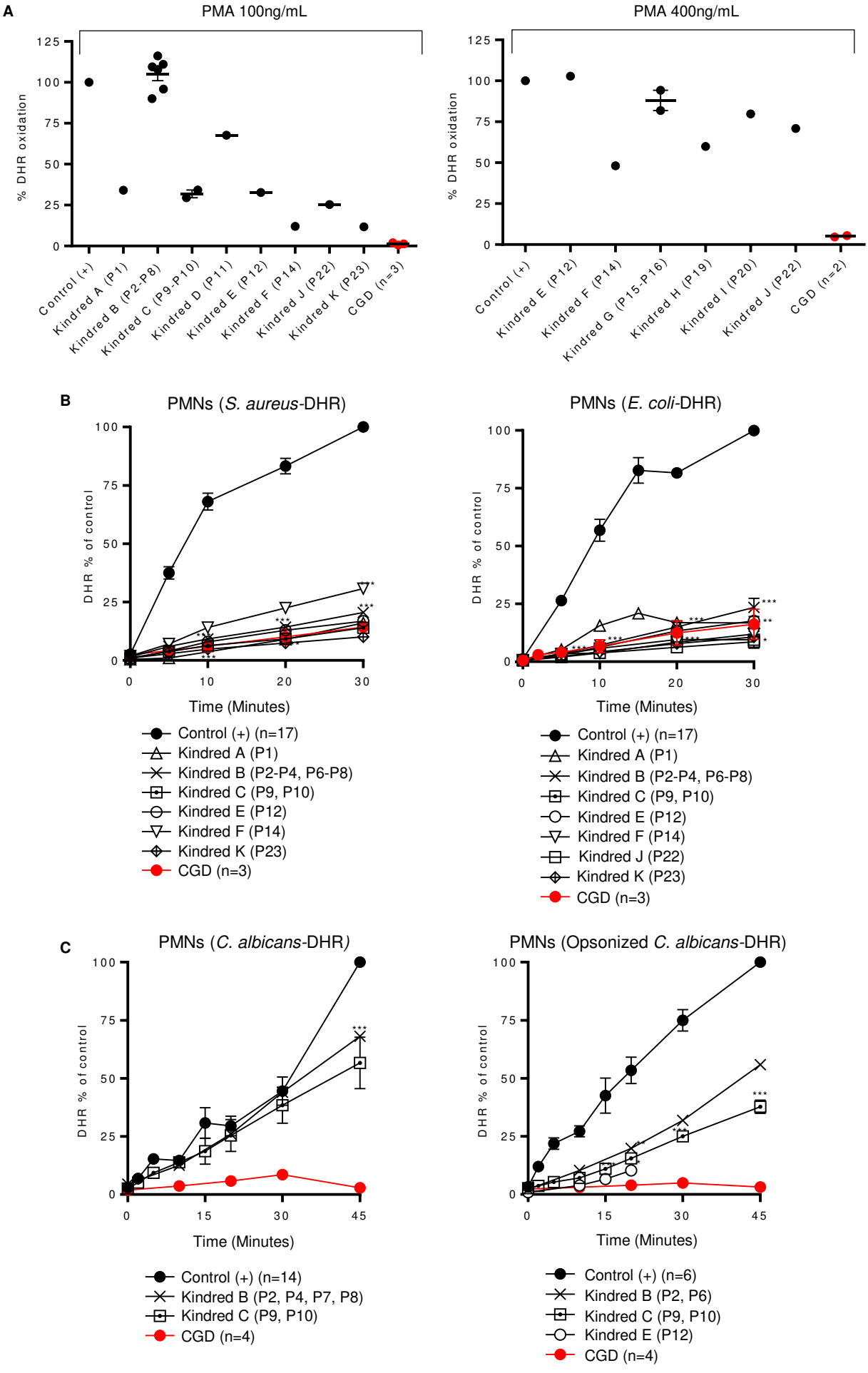
A
PMA 100ng/mL
% DHR oxidation
Control (+)
Kindred A (P1)
Kindred B (P2-P8)
Kindred C (P9-P10)
Kindred D (P11)
Kindred E (P12)
Kindred F (P14)
Kindred J (P22)
Kindred K (P23)
CGD (n=3)
PMA 400ng/mL
% DHR oxidation
Control (+)
Kindred E (P12)
Kindred F (P14)
Kindred G (P15-P16)
Kindred H (P19)
Kindred I (P20)
Kindred J (P22)
CGD (n=2)
B
PMNs (S. aureus-DHR)
DHR % of control
Time (Minutes)
Control (+) (n=17)
Kindred A (P1)
Kindred B (P2-P4, P6-P8)
Kindred C (P9, P10)
Kindred E (P12)
Kindred F (P14)
Kindred K (P23)
CGD (n=3)
PMNs (E. coli-DHR)
DHR % of control
Time (Minutes)
Control (+) (n=17)
Kindred A (P1)
Kindred B (P2-P4, P6-P8)
Kindred C (P9, P10)
Kindred E (P12)
Kindred F (P14)
Kindred J (P22)
Kindred K (P23)
CGD (n=3)
C
PMNs (C. albicans-DHR)
DHR % of control
Time (Minutes)
Control (+) (n=14)
Kindred B (P2, P4, P7, P8)
Kindred C (P9, P10)
CGD (n=4)
PMNs (Opsonized C. albicans-DHR)
DHR % of control
Time (Minutes)
Control (+) (n=6)
Kindred B (P2, P6)
Kindred C (P9, P10)
Kindred E (P12)
CGD (n=4)

Figure 4

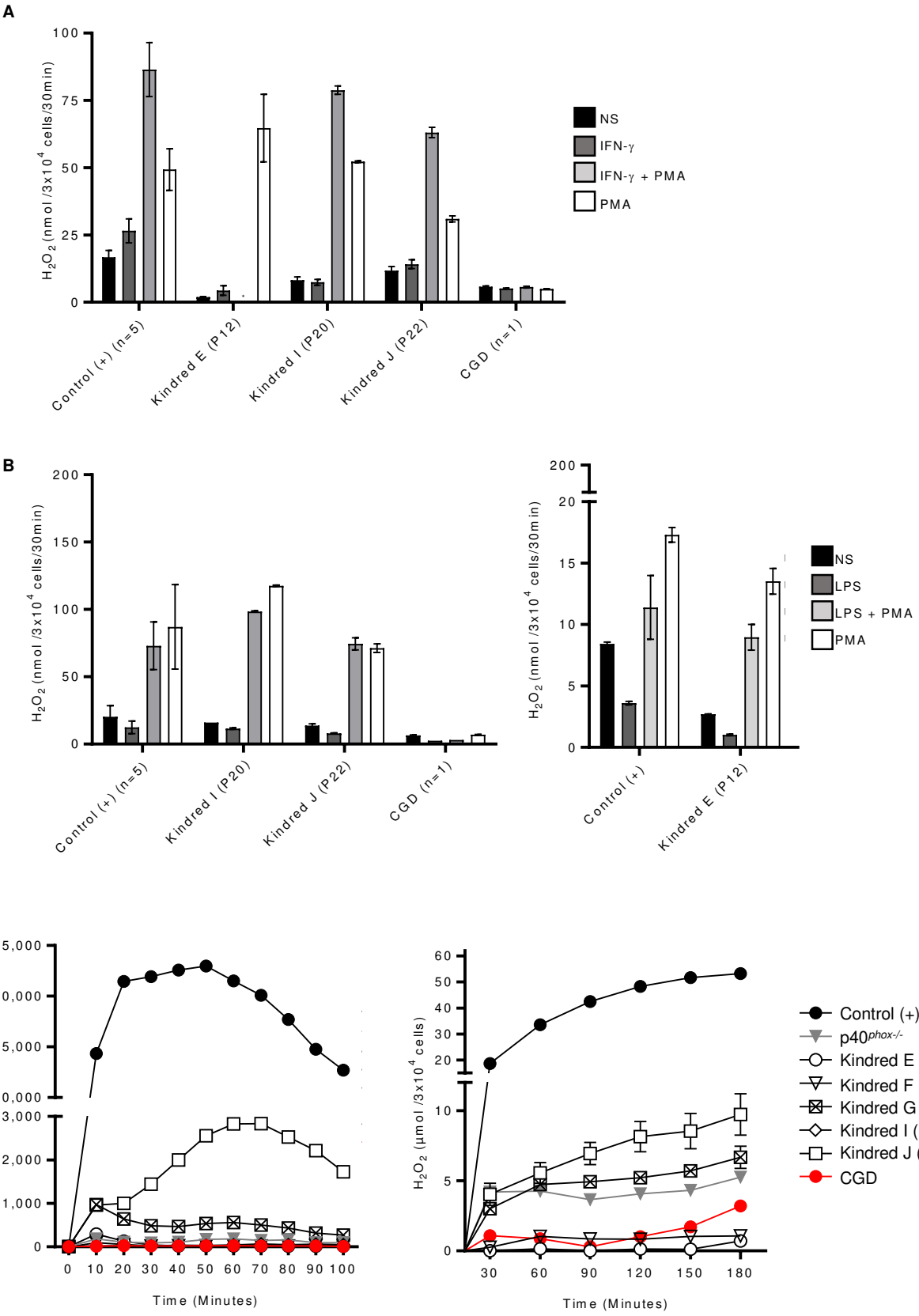
A
100
75
50
25
0
H_2O_2 (nmol /3x10^4 cells/30min)
NS
IFN-γ
IFN-γ + PMA
PMA
Control (+) (n=5)
Kindred E (P12)
Kindred I (P20)
Kindred J (P22)
CGD (n=1)
B
200
150
100
50
0
H_2O_2 (nmol /3x10^4 cells/30min)
Control (+) (n=5)
Kindred I (P20)
Kindred J (P22)
CGD (n=1)
200
20
15
10
5
0
H_2O_2 (nmol /3x10^4 cells/30min)
NS
LPS
LPS + PMA
PMA
Control (+)
Kindred E (P12)
C
25,000
20,000
15,000
10,000
3,000
2,000
1,000
0
LU x 10^3
0 10 20 30 40 50 60 70 80 90 100
Time (Minutes)
60
50
40
30
20
10
5
0
H_2O_2 (µmol /3x10^4 cells)
30 60 90 120 150 180
Time (Minutes)
Control (+)
p40$^{phox-/-}$
Kindred E (P12)
Kindred F (P14)
Kindred G (P15)
Kindred I (P20)
Kindred J (P22)
CGD

Figure 5

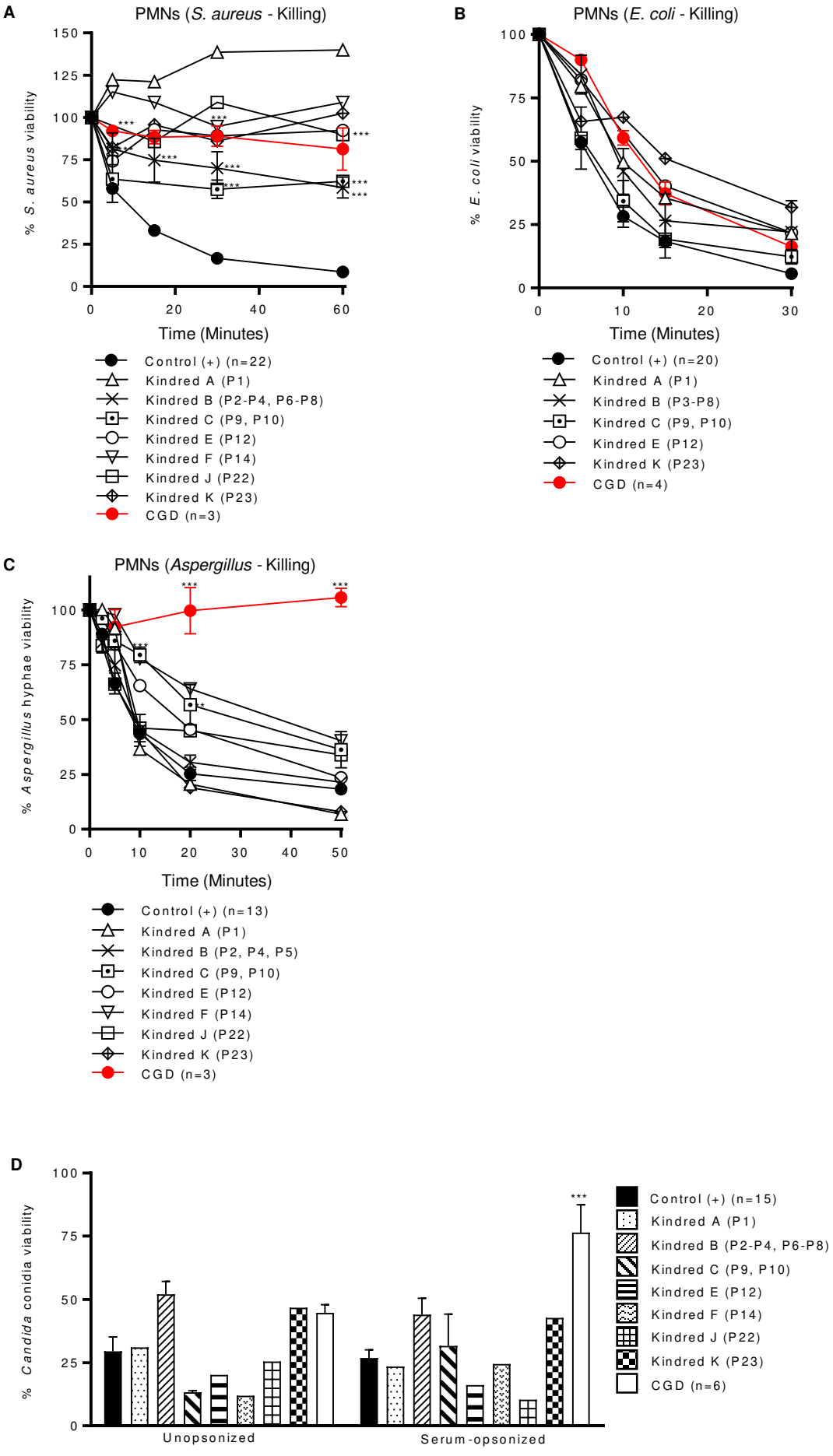
A
PMNs (S. aureus - Killing)
% S. aureus viability
Time (Minutes)
Control (+) (n=22)
Kindred A (P1)
Kindred B (P2-P4, P6-P8)
Kindred C (P9, P10)
Kindred E (P12)
Kindred F (P14)
Kindred J (P22)
Kindred K (P23)
CGD (n=3)
B
PMNs (E. coli - Killing)
% E. coli viability
Time (Minutes)
Control (+) (n=20)
Kindred A (P1)
Kindred B (P3-P8)
Kindred C (P9, P10)
Kindred E (P12)
Kindred K (P23)
CGD (n=4)
C
PMNs (Aspergillus - Killing)
% Aspergillus hyphae viability
Time (Minutes)
Control (+) (n=13)
Kindred A (P1)
Kindred B (P2, P4, P5)
Kindred C (P9, P10)
Kindred E (P12)
Kindred F (P14)
Kindred J (P22)
Kindred K (P23)
CGD (n=3)
D
% Candida conidia viability
Unopsonized
Serum-opsonized
Control (+) (n=15)
Kindred A (P1)
Kindred B (P2-P4, P6-P8)
Kindred C (P9, P10)
Kindred E (P12)
Kindred F (P14)
Kindred J (P22)
Kindred K (P23)
CGD (n=6)

Figure 6

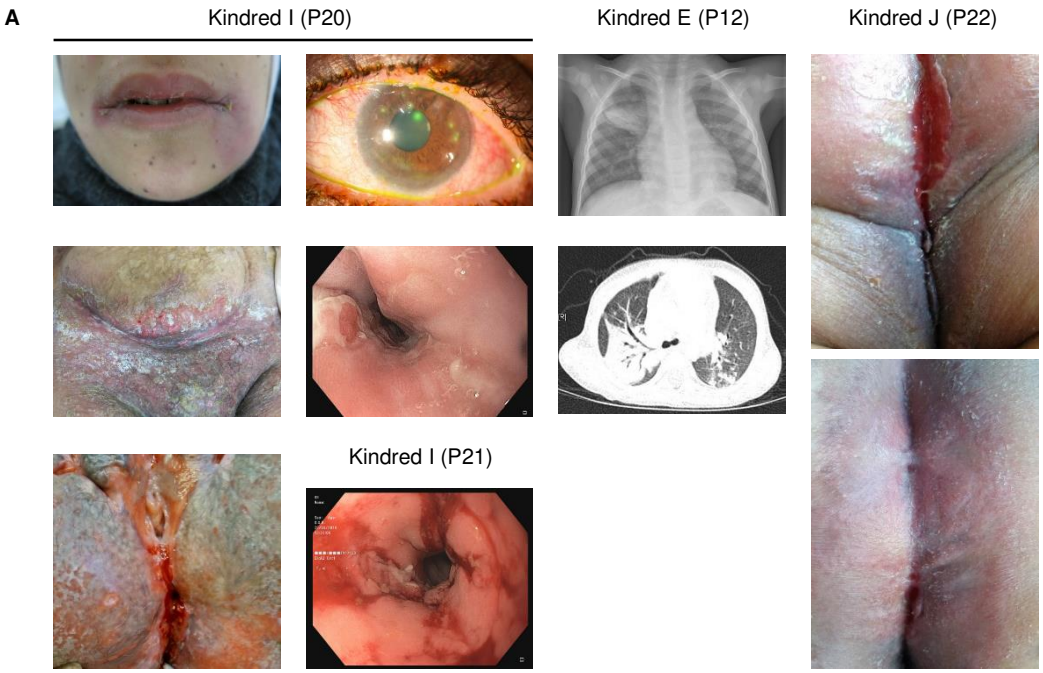
A
Kindred I (P20)
Kindred E (P12)
Kindred J (P22)
Kindred I (P21)

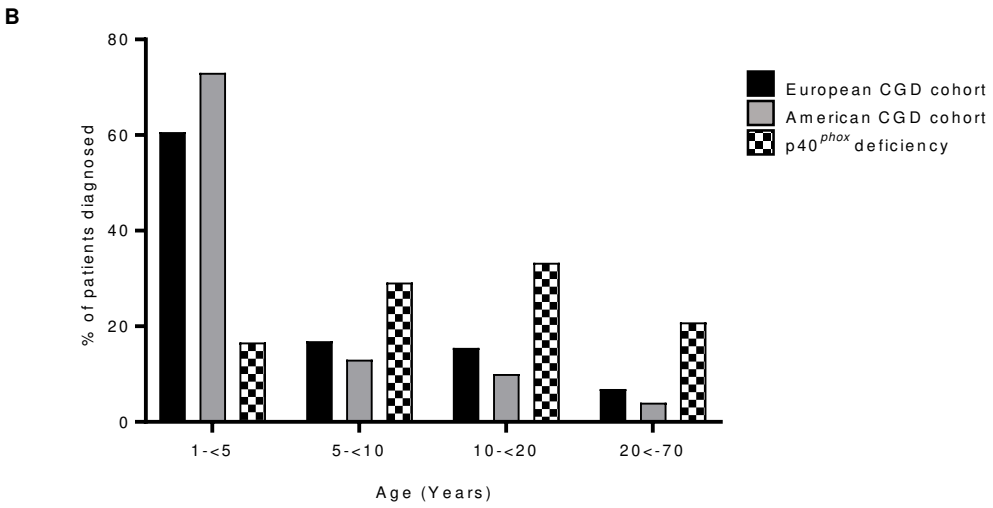
B
80
60
40
20
0
% of patients diagnosed
European CGD cohort
American CGD cohort
p40phox deficiency
1-<5
5-<10
10-<20
20<-70
Age (Years)

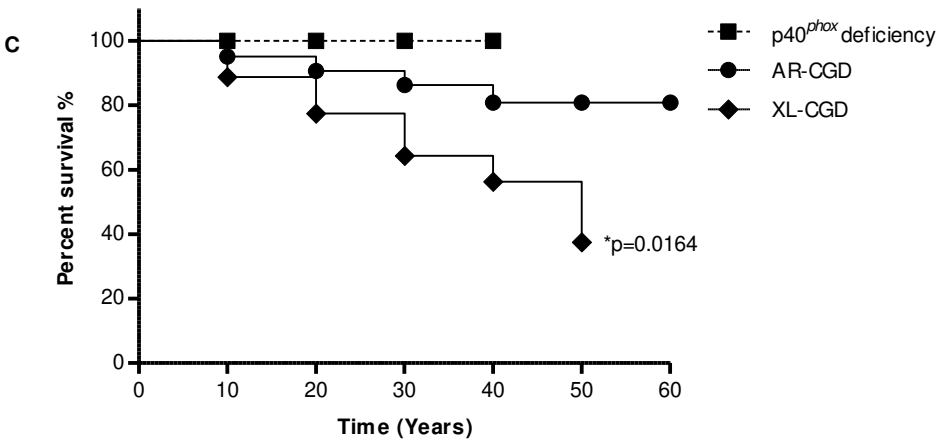
C
100
80
60
40
20
0
Percent survival %
p40phox deficiency
AR-CGD
XL-CGD
*p=0.0164
0
10
20
30
40
50
60
Time (Years)

Figure 7

Figure legends

Figure 1. Identification of *NCF4* mutations. (**A**) Pedigrees of 12 families showing allele segregation. The index cases are indicated by an arrow, and "E?" indicates an unknown genotype, black or white filled symbols represent individuals with and without clinical manifestations, respectively. WT: wild type; m: mutated. Triangles represent pregnancies not carried to term. **(B)** Schematic diagram of the structure of the *NCF4* gene and p40^{phox} protein, consisting of 9 exons and three protein domains, respectively. Newly discovered and previously reported mutations of the *NCF4* gene are noted according to their localization.

Figure 2. p40^{phox} levels and NADPH oxidase activity of the *NCF4* mutated alleles

(A) Western blot of total protein extracts from HEK293T cells expressing *NCF4* cDNAs. The upper panel data were obtained with a polyclonal anti-p40^{phox} antibody and the lower panel data were obtained with an anti-Flag-DDK antibody. An antibody against GAPDH was used as a loading control. **(B)** Western blot of total protein extracts from healthy control and *NCF4*$^{-/-}$ EBV-B cells retrovirally transduced with *NCF4* cDNAs. A polyclonal anti-p40^{phox} antibody was used, with an antibody against GAPDH as the loading control. NT, not transduced; EV, empty vector. **(C)** Production of superoxide (O_2^-) by *NCF4*$^{-/-}$ EBV-B cells retrovirally transduced with *NCF4* cDNAs, upon PMA stimulation. The results shown are representative of two independent assays. **(D)** DHR reaction of NB4 p40^{phox} KO cells stimulated with PMA. **(E)** or with *E. coli* stimulation. **(F)** Killing activity of NB4 p40^{phox} KO cells infected with *S. aureus*. N=2-3. 2-Tailed Mann U Whitney test. Data represent mean + SEM when N≥3 or mean only when N<3.

Figure 3. p40^{phox} and NADPH oxidase subunit expression in p40^{phox}-deficient cells. (**A**) Western blot of total protein extracts from the neutrophils of healthy controls, patients and

heterozygous relatives. Antibodies against p40^{phox} protein were used. Actin or GAPDH protein was used as a loading control. **(B)** Western blot of total protein extracts from MDMs and MDDCs from a healthy control and p40^{phox}-deficient patients. Detection with polyclonal anti-p40^{phox} antibody and antibody against GAPDH as a loading control. **(C)** Western blot of total extracts from EBV-B cells from a healthy control, p40^{phox}-deficient patients, XR and AR CGD patients. Antibodies against p40^{phox} protein or gp91^{phox}, p22^{phox}, p67^{phox} and p47^{phox} were used. Actin or GAPDH protein was used as loading control. **(D)** Intracellular detection of gp91^{phox}, p22^{phox}, p67^{phox} and p47^{phox} in EBV-B cells from a healthy control, p40^{phox}-deficient patients, XR and AR CGD patients. The results shown are representative of two independent assays. p40$^{phox-/-}$ indicates a patient reported in a previous study (26).

Figure 4. NADPH oxidase activity in p40^{phox}-deficient neutrophils. (A) Intracellular ROS production by DHR in neutrophils from healthy controls (*n*=37), p40^{phox}-deficient patients (*n*=17) and CGD patients (*n*=5) upon PMA stimulation (left panel: 100 ng PMA/mL) and (right panel: 400 ng/µL). **(B)** Particle-induced DHR oxidation in neutrophils from healthy controls (*n*=17 and *n*=23), p40phox-deficient patients (*n*=12 and *n*=14) and CGD patients (*n*=3 and *n*=6) upon stimulation with *S. aureus* (left) and *E. coli* (right). **(C)** DHR oxidation in neutrophils from healthy controls (*n*=14 and *n*=6), p40^{phox}-deficient patients (*n*=6 and *n*=5) and CGD patients (*n*=4 and *n*=3) upon addition of *C. albicans,* with (left) or without (right) opsonization.

Figure 5. NADPH oxidase activity in p40^{phox}-deficient mononuclear cells. (A) Extracellular H_2O_2 production by MDMs from healthy controls (*n*=5), p40^{phox}-deficient patients (*n*=3) and CGD patients (*n*=1) upon PMA stimulation; cells with and without IFN-γ priming. **(B)** Extracellular H_2O_2 production by MDDCs from healthy controls (*n*=5), p40^{phox}-deficient

patients (*n*=3) and CGD patients (*n*=1) upon PMA stimulation; cells with and without LPS priming. **(C)** Production of O_2^- (left) and release of H_2O_2 (right) by EBV-B cells from healthy controls (*n*=2), p40^{phox}-deficient patients (*n*=6) and CGD patients (*n*=1) upon PMA stimulation, assessed on the basis of luminol bioluminescence or Amplex Red. The results shown are representative of two independent assays.

Figure 6. Pathogen killing activity by neutrophils from p40^{phox}-deficient patients. (A) *S. aureus* viability measured with infected neutrophils from healthy controls (*n*=22), p40^{phox}-deficient patients (*n*=13) and CGD patients (*n*=3). **(B)** *E. coli* viability measured with infected neutrophils from healthy controls (*n*=20), p40^{phox}-deficient patients (*n*=10) and CGD patients (*n*=4). **(C)** *A. fumigatus* hypha viability measured at different time points with infected neutrophils from healthy controls (*n*=13), p40^{phox}-deficient patients (*n*=13) and CGD patients (*n*=3). **(D)** *C. albicans* conidial viability measured with infected neutrophils from healthy controls (*n*=15), p40^{phox}-deficient patients (*n*=12) and CGD patients (*n*=6). 2-Tailed Mann U Whitney test. Data represent mean + SEM when N≥3 or mean only when N<3. *p<0.05, ** p<0.01 and *** p<0.001. For Figure **(D)** the Bonferroni correction for multiple comparisons was applied and an adjusted p value of <0.0063 was considered significant (*) and *** p<0.001.

Figure 7. Clinical manifestation and outcome of p40^{phox} deficient patients. (A) P20: Cheilitis, episcleritis, severe chronic cutaneous lesions, esophagitis. P21: Esophagitis. P12: Multifocal consolidations and infiltrates in both lungs on X ray and thorax CT-scan. P22: Vulvar lichen planus before (upper panel) and after (lower panel) steroid treatment. **(B)** Distribution of age at CGD diagnosis in an American (USA) and a European cohort [(7) and (9) references] and in the p40^{phox}-deficient patients in this study. **(C)** Kaplan-Meier survival

curve compiling CGD patients *n*=363 (XR *n*=240 and AR *n*=123) from (7) and (19) references, and the p40^{phox}-deficient patients studied here.

Table 1. The clinical spectrum of p40^{phox} deficiency

Table 1. The clinical spectrum of p40^{phox} deficiency

Kindred	Patient	Mutation	Consanguinity	Origin	Sex (F/M)	Follow-up	Age at onset of symptoms (years)	Age at CGD diagnosis (years)	Clinical phenotype (infections, autoimmunity, microbiology, imaging, pathology results) Prophylaxis/current treatment; HSCT
A	P1 (II.1)	c.1181G>A/ 118-1G>A	Yes	Pakistan (living in UK)	M	Alive	4	9	Mouth ulcers, IBD with colonic granulomata, poorly responsive to mesalazine; *S. aureus* skin abscesses. ANA-negative. BCG vaccination with no AE. Prophylaxis: cotrimoxazole/itraconazole.
B	P2 (IV.7)	p.R105Q/ R105Q	Yes	Pakistan (living in UK)	F	Alive	9	14	Lupus-like skin lesions, no IBD symptoms. ANA-negative. Prophylaxis: cotrimoxazole/itraconazole
	P3 (III.1)				M	Alive	unknown	46	Lupus-like skin lesions in childhood. ANA/anti-dsDNA antibody-negative. Prophylaxis: none
	P4 (IV.1)				M	Alive	5	23	Recurrent MRSA skin infections, eczema. ANA-negative. Prophylaxis: none
	P5 (IV.4)				M	Alive	unknown	19	Non-necrotizing granulomatous inflammation of the gums and skin. AFB/fungus-negative. ANA-negative. Prophylaxis: none
	P6 (IV.5)				M	Alive	7	16	Recurrent skin infections; lupus-like skin lesions; seborrheic dermatitis. Prophylaxis: cotrimoxazole/itraconazole
	P7 (IV.6)				F	Alive	3	15	Impetigo; discoid lupus. SM, GPC, mitochondrial defects, reticulin, LKM-negative Prophylaxis: cotrimoxazole/itraconazole/hydroxychloroquine
	P8 (IV.9)				F	Alive	4	9	Skin abscesses (MRSA/GBS), impetigo; lupus-like skin lesions. ANA, DNAq, ANCA, TPO, C1q antibodies: negative. Prophylaxis: cotrimoxazole/itraconazole/hydroxychloroquine
C	P9 (II.1)	c.120_134del/120_134del	No	Portugal	M	Alive	5	7	Dental and cutaneous abscesses; periodontitis. BCG vaccination with no AE. Prophylaxis: cotrimoxazole/itraconazole.
	P10 (II.2)				F	Alive	1	1	Recurrent oral ulcers, no IBD symptoms. BCG vaccination with no AE. Prophylaxis: cotrimaxozole/itraconazole.
D	P11 (II.1)	c.118-1G>A/ c.759-1G>C	No	USA	M	Alive	7	10	Cutaneous discoid lupus erythematosus complicated by *S. aureus* skin infection; anal fissures, mouth ulcers, cryptitis in descending colon, sigmoid and rectum. Prophylaxis: none; post-HSCT

E	P12 (II.3)	c.118-1G>A/ 118-1G>A	Yes	Pakistan (living in UK)	F	Alive	1	2	Chronic fever, recurrent pulmonary infections (no positive cultures). Lung, lymph node Granulomata. ANA, ANCA, ENAs dsDNA antibodies: negative. Cardiolipin G 87.6 GPLU (0 - 5.7) Prophylaxis: cotrimoxazole and itraconazole
	P13 (II.4)				M	Alive	-	1	Asymptomatic Prophylaxis: cotrimoxazole and itraconazole
F	P14 (II.5)	c.32+2T>G/ 32+2T>G	Yes	Pakistan (living in UK)	F	Alive	2	5	Recurrent respiratory infections (BAL: viruses and *Candida*), bronchiectasis. Bilateral dense consolidation on lung CT. Chronic interstitial inflammation on lung biopsy, successfully treated with an IV pulse of methylprednisolone. Lymphadenitis with abscesses C-ANCA- and ANA-positive. Prophylaxis: cotrimoxazole/itraconazole. In work-up for HSCT
G	P15 (II.5)	p.R58C/R58C	No	Colombia	M	Alive	2	6	Chronic fever. Chronic diarrhea. Oral thrush (no microbiology results). Recurrent disseminated histoplasmosis (lymph nodes, FCS, liver, spleen, serum, urine, bone marrow), successfully treated with amphotericin B, itraconazole and fluconazole. BCG-vaccine: no AE. Prophylaxis: cotrimoxazole/itraconazole
	P16 (II.3)				M	Alive	-	10	Asymptomatic. BCG vaccine with no AE. Prophylaxis: none
	P17 (II.4)				F	Alive	-	8	Asymptomatic. BCG vaccine with no AE. Prophylaxis: none
	P18 (II.8)				M	Alive	-	3	Asymptomatic. BCG vaccine with no AE. Prophylaxis: none
H	P19 (II.1)	p.P144T/ P144T	No	Argentina	F	Alive	1	7	Pneumonia. Regional lymphadenitis (BCG-itis). Cutaneous lesions (granulomatous, no organisms detected, stains/PCR not available). Meningitis due to *M. avium* complex. Prophylaxis: none
I	P20 (II.1)	p.W239X/ W239X	Yes	Kuwait (living in Belgium)	F	Alive	14	37	Gastritis, severe complex perianal fistula with recurrent abscesses and anal stenosis. Adenocarcinoma of anal canal. Treatment: steroids, azathioprine, infliximab, golimumab. Chemo- and radiotherapy for adenocarcinoma. Prophylaxis: none, post-HSCT
	P21 (II.3)				F	Alive	8	32	Esophageal ulcerations and severe perianal fistula diagnosed as Crohn's disease. Recurrent skin abscesses. Episcleritis. Severe periodontitis. Treatment: steroids, adalimumab, high-dose proton pump inhibitors Prophylaxis: none, post-HSCT
J	P22 (II.2)	c.120_134 del/120-134del	No	Portugal	F	Alive	2	15	IBD with granuloma in colon. Vulvar lichen planus (at 2 years old). Pilonidal cyst surgery. ASCA-positive. BCG vaccine with no AE. Treatment: steroids, infliximab, adalimumab, thalidomide Prophylaxis: cotrimoxazole
K	P23 (II.4)	c.118-1G>A/ 118-1G>A	No	Russia (born in Germany)	F	Alive	11	17	IBD with granulomata in oral mucosa, esophagus and colon. Recurrent blepharitis/conjunctivitis. Treatment: steroids, MTX, ustekinumab; exclusive enteral nutrition, mesalazine, azathioprine, tacrolimus, colchicine, interferon-gamma, adalimumab and/or anakinra were ineffective. Prophylaxis: cotrimoxazole

L	P24 (II.3)	p.R58C/R58C	No	Chile	F	Alive	17	23	IBD with colonic granulomata and severe perianal disease. Erythema nodosum and pyoderma gangrenosum. Treatment: ciprofloxacin, mesalamine, and prednisolone. Chronic, refractory disease despite escalating immunomodulatory (azathioprine, 6MP), and biological (adalimumab, infliximab, natalizumab) drugs. Total colectomy with ileostomy; return of symptoms post-surgery. Infliximab. Prophylaxis: none

6MP: 6-mercaptopurine; AE: adverse effect; AFB : acid-fast bacilli, ANA: antinuclear antibodies; ANCA: anti-neutrophil cytoplasmic antibody; ASCA: anti-*Saccharomyces cerevisiae* antibodies; BAL: bronchoalveolar lavage; BCG: bacillus Calmette-Guérin; CT: computed tomography; ds-DNA: double-stranded (ds, native) DNA; HSCT: hematopoietic stem cell transplantation; IBD: inflammatory bowel disease; LKM: anti-liver-kidney microsomal antibody; MRSA/GBS: methicillin-resistant *Staphylococcus aureus*/group B *Streptococcus*; MTX: methotrexate; TPO: thyroperoxidase antibodies